

SOLID21

VP5 Plasmatic technologies

VP5 leader

Zdeněk Hubička



FZU

Fyzikální ústav
Akademie věd
České republiky

The project Solid state physics for the 21st century – SOLID21
CZ.02.1.01/0.0/0.0/16_019/0000760 is co-funded by the European Union.



EVROPSKÁ UNIE
Evropské strukturální a investiční fondy
Operační program Výzkum, vývoj a vzdělávání



Research program Plasmatic Technologies (RP 5)

head Zdeněk Hubička

RP5 is composed of six Research activities (RA):

RA1- R&D of advanced low temperature plasma systems for thin film polycrystalline materials (Z. Hubička)

RA2 - Plasma diagnostics, optimization of plasma deposition systems, and monitoring of deposition processes (M. Čada)

RA3 - Plasma methods of preparation of thin metallic and intermetallic layers (J. Lančok)

RA4 - Thin-film chemical sensors (M. Novotný)

RA5 – Optical materials-plasmon structures (J. Bulíř)

RA6 – Structures exhibiting a combination of ferromagnetic properties (M. Tjunina)

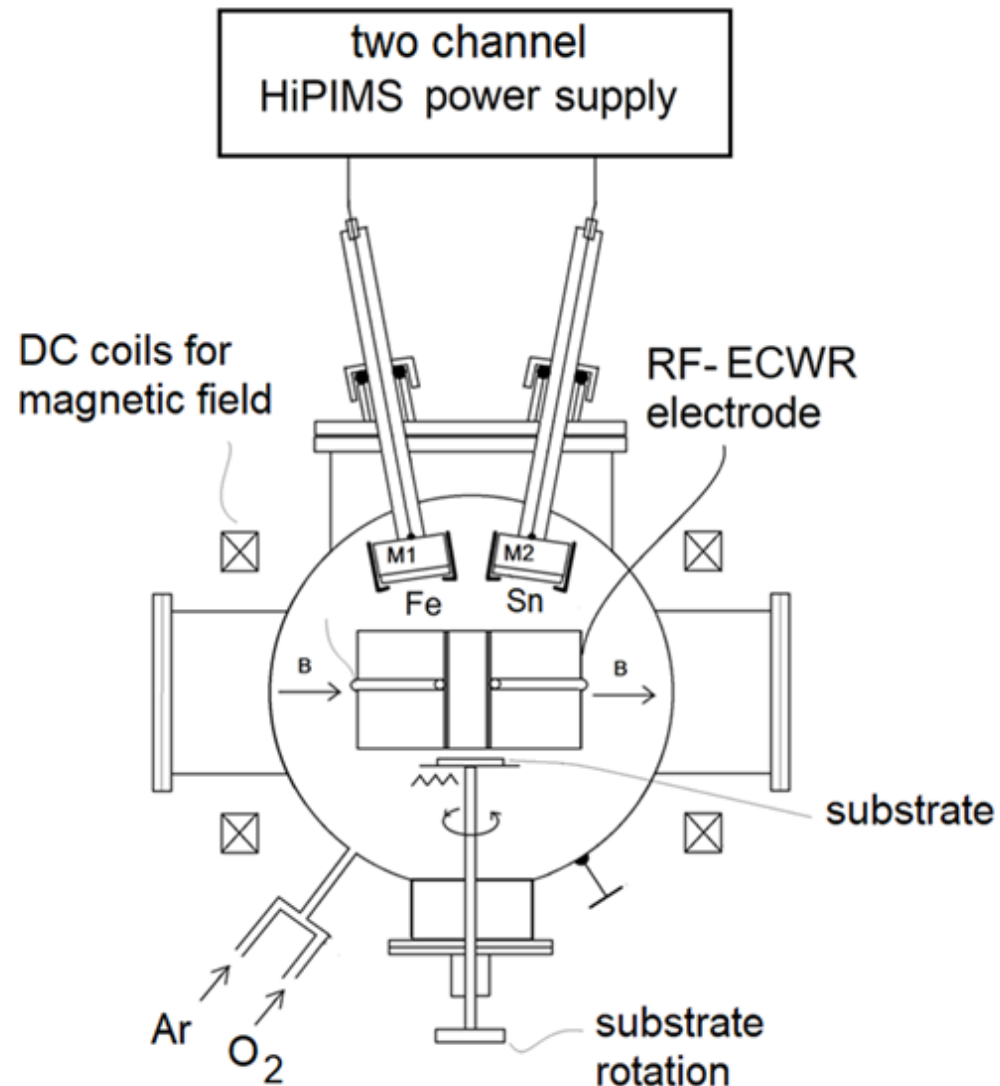
Research program 1 R&D of advanced low temperature plasma systems for thin film polycrystalline materials

RP leader

Zdeněk Hubička

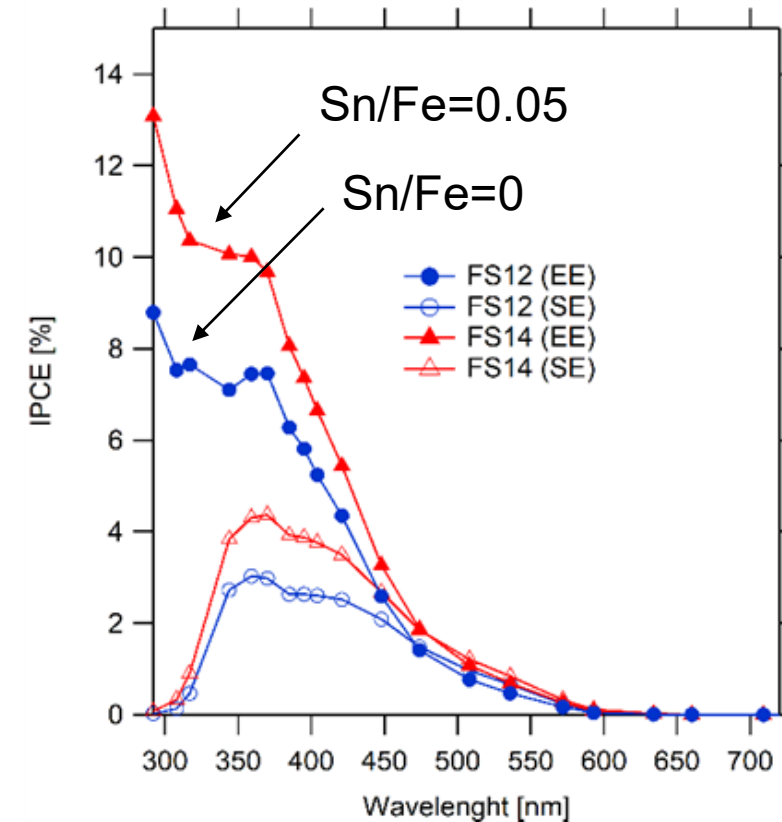
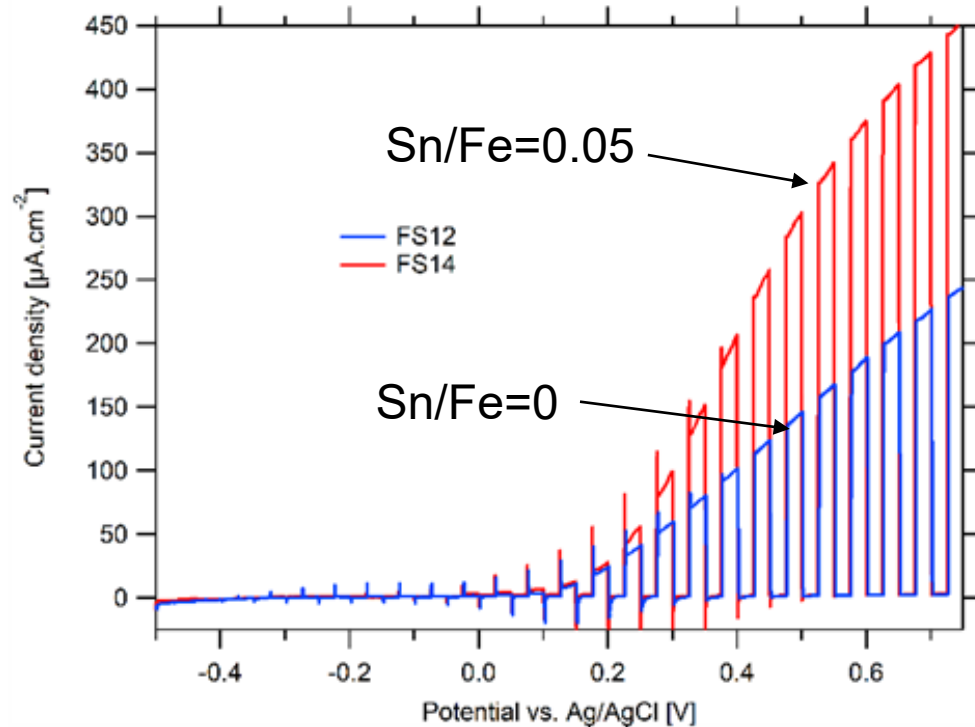
- semiconductor oxides (doped, ternary) deposited by reactive pulsed HiPIMS plasma systems are investigated for solar water splitting and hydrogen production
- ZnO semiconductor thin films deposited by plasma systems for fast photon detectors cooperation with Institute of Laser Engineering in Osaka university Japan (Marilou Catadal Raduban, Nobuhiko Sarukura, Kohei Yamanoi)
- unipolar and bipolar pulsed linear hollow cathode sputtering plasma jet was developed and sold as prototype to IQS group, s.r.o. as a deposition source implemented in large industrial roll to roll coater
- new plasma machines for pulsed reactive sputtering of sulphides and selenides was already finished. Polycrystalline LuS_2 , MoS_2 semiconductor thin films were deposited for photonic applications

Deposition of $\text{Fe}_2\text{O}_3\text{:Sn}$ semiconducting (n-type) thin films by reactive pulsed r-HiPIMS + ECWR co-sputtering from Fe and Sn target. (to be published with VSCHT and J. Heyrovsky institute of Physical Chemistry CAS)



Deposition of $\text{Fe}_2\text{O}_3\text{:Sn}$ semiconducting (n-type) thin films by reactive pulsed r-HiPIMS + ECWR co-sputtering from Fe and Sn target

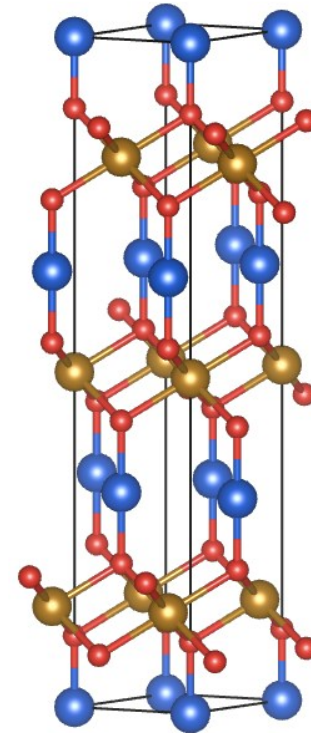
PEC measurements (photoanode)



LSV, chopped-light 5 s dark/ 5 s light, scan rate 5 mV/s, Light source UV diode, intensity 100 W/m², electrolyte/electrode illumination, electrolyte: 0.1M NaOH of samples FS12 and FS14 deposited on FTO electrode.

Photocathode p-type semiconductor CuFeO_2 with delafossite structure

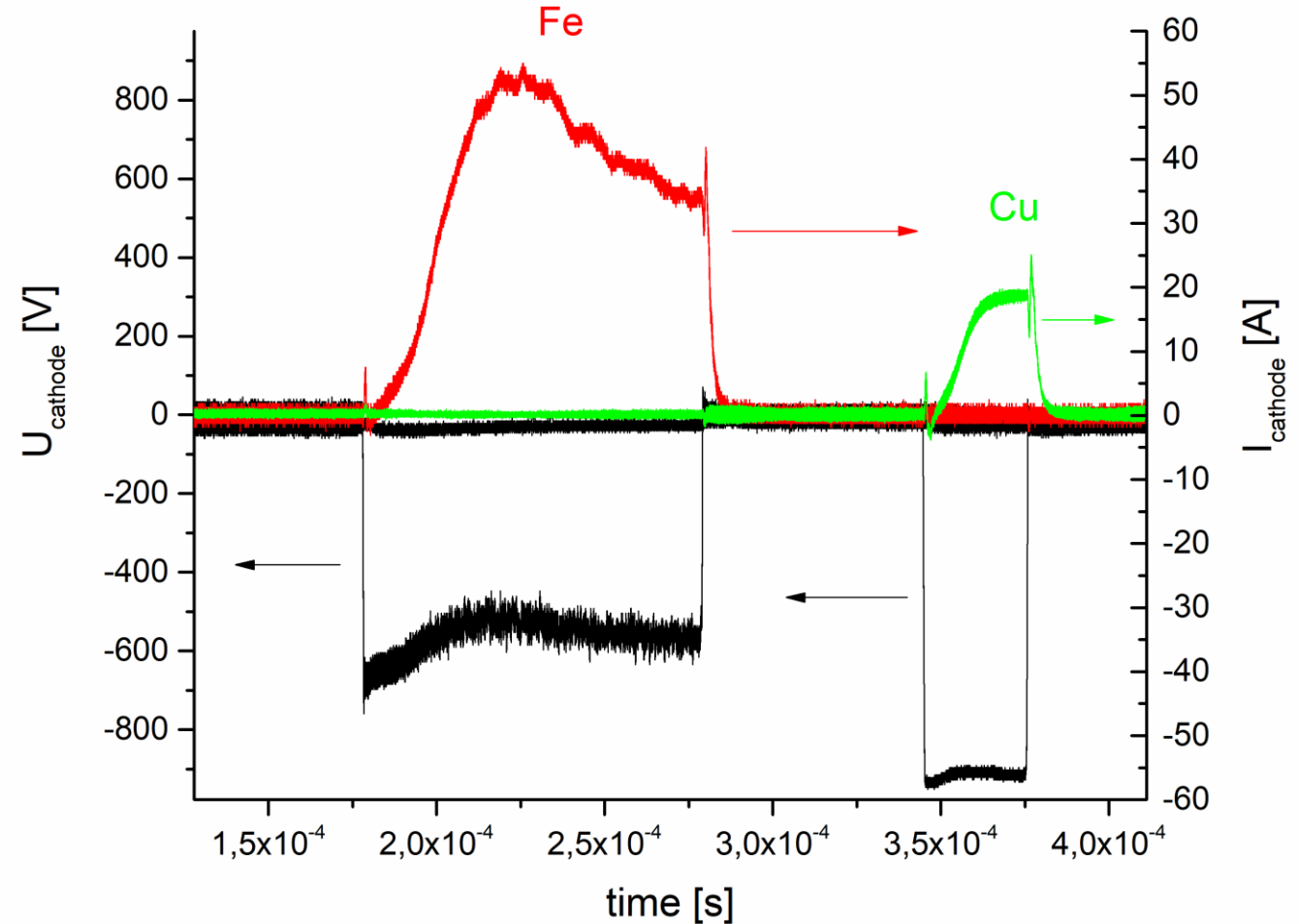
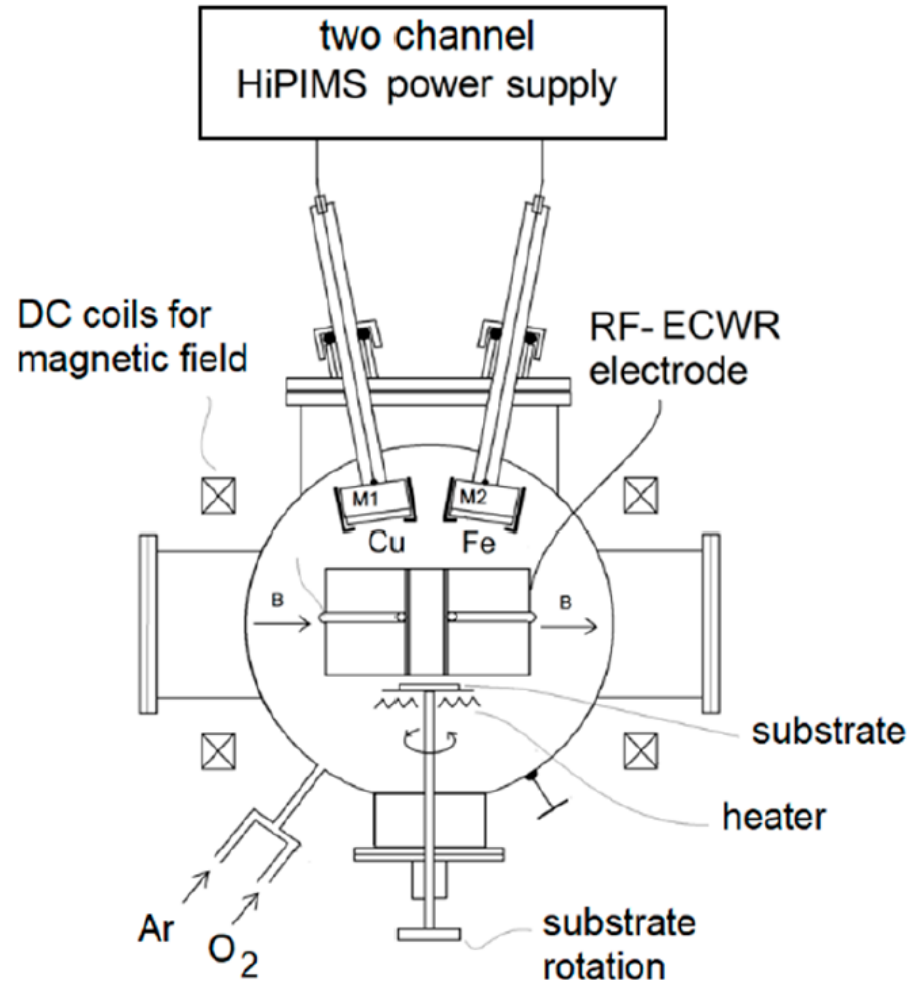
- cooperation with University of Greifswald
- exceptional stability in basic aqueous electrolyte
- favorable band gap $E_g = 1.47 \text{ eV}$
- earth-abundant component (Cu, Fe, O)
- disadvantage - small photocurrents (needs improvement)



HiPIMS or HiPIMS+ECWR with dual magnetron for alloy and multicomponent thin films $\text{Cu}_{1+y}\text{FeO}_x$

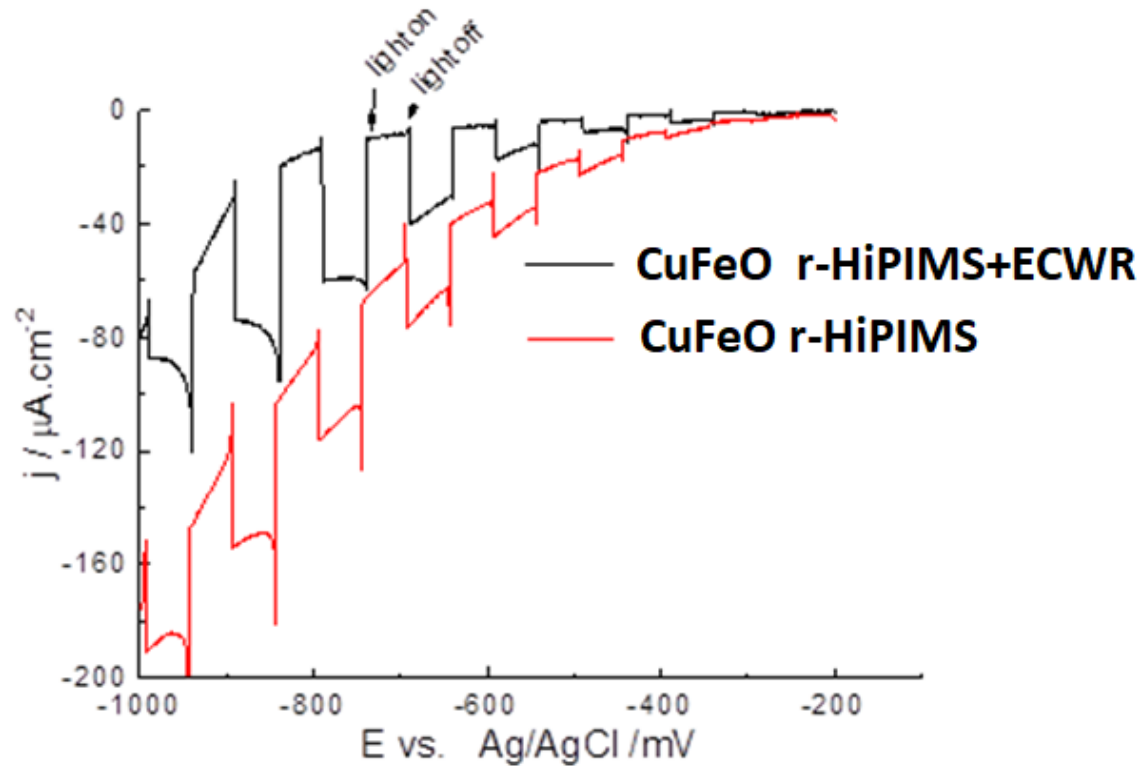
7

(semiconducting films: $\text{Cu}_{1+y}\text{FeO}_x$)

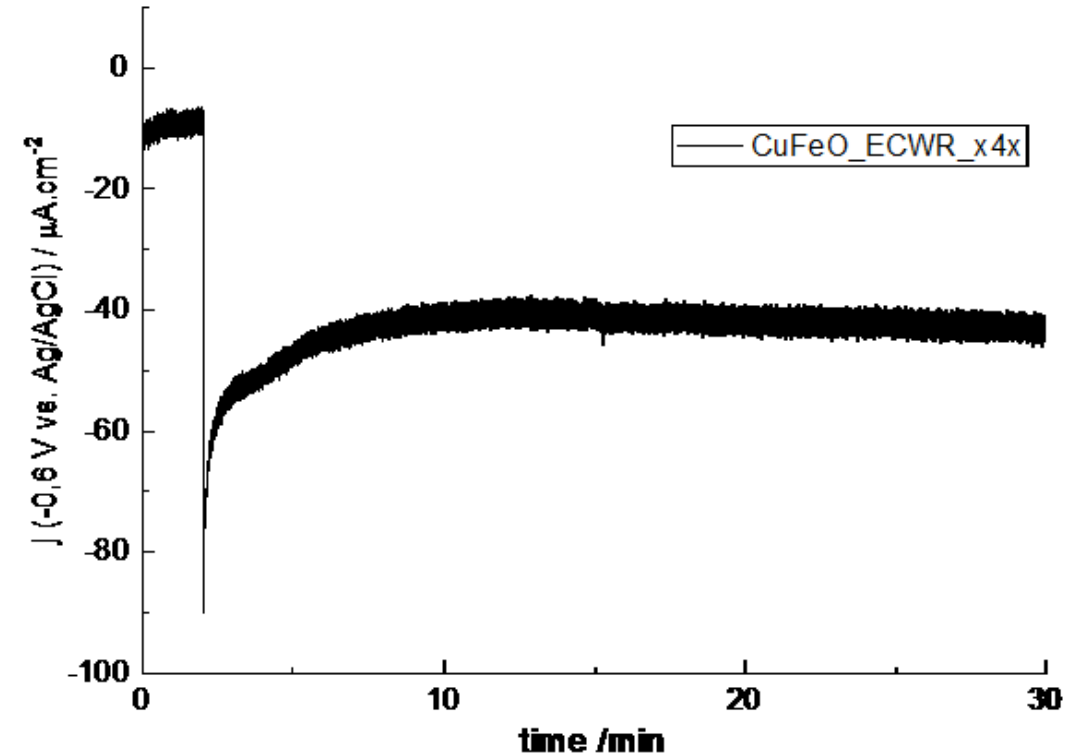


Plasma diagnostics by RF planar probe during the deposition process

Deposition of CuFeO_2 with Cu and Fe target in $\text{Ar}+\text{O}_2$ gas mixture (A. Písaříková, et. al. to be published)



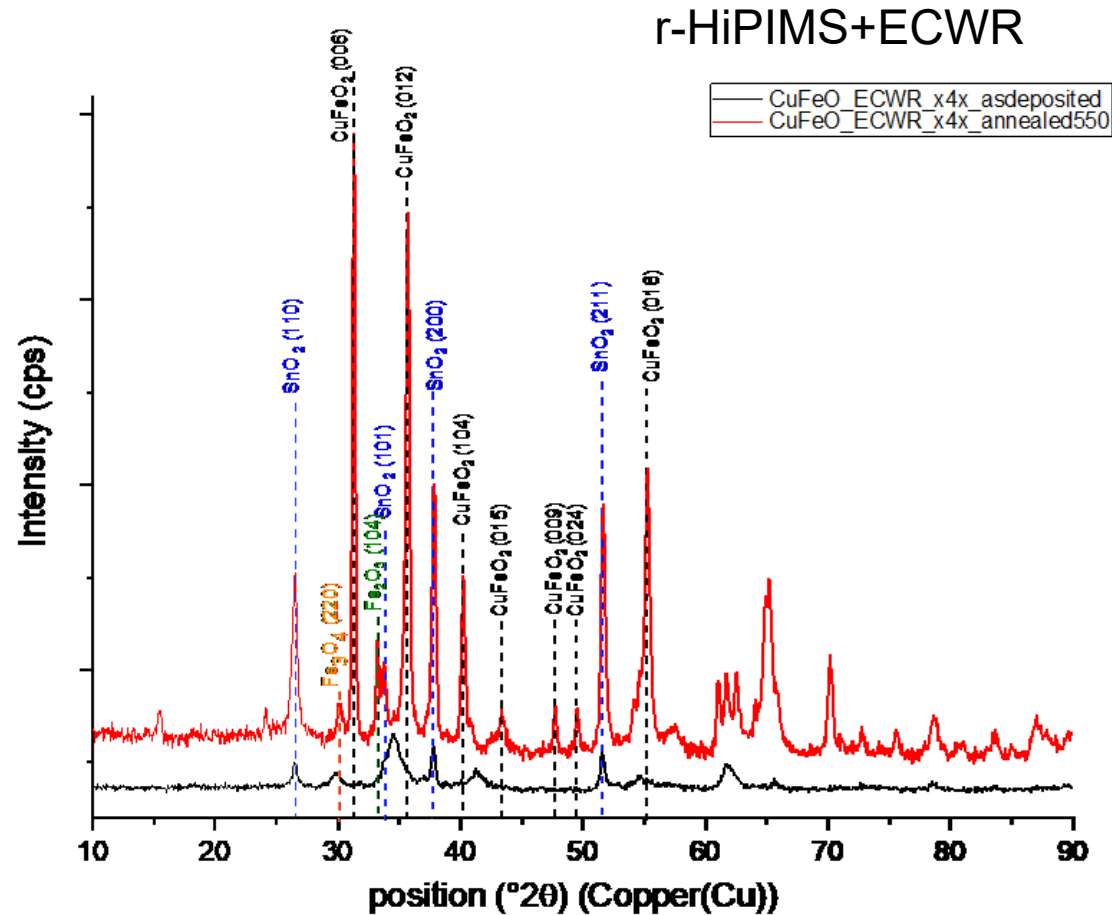
Cycled polarization curves of CuFeO_2 prepared by r-HiPIMS, r-HiPIMS+ECWR, annealed at 550°C , in 1 mol/l NaOH



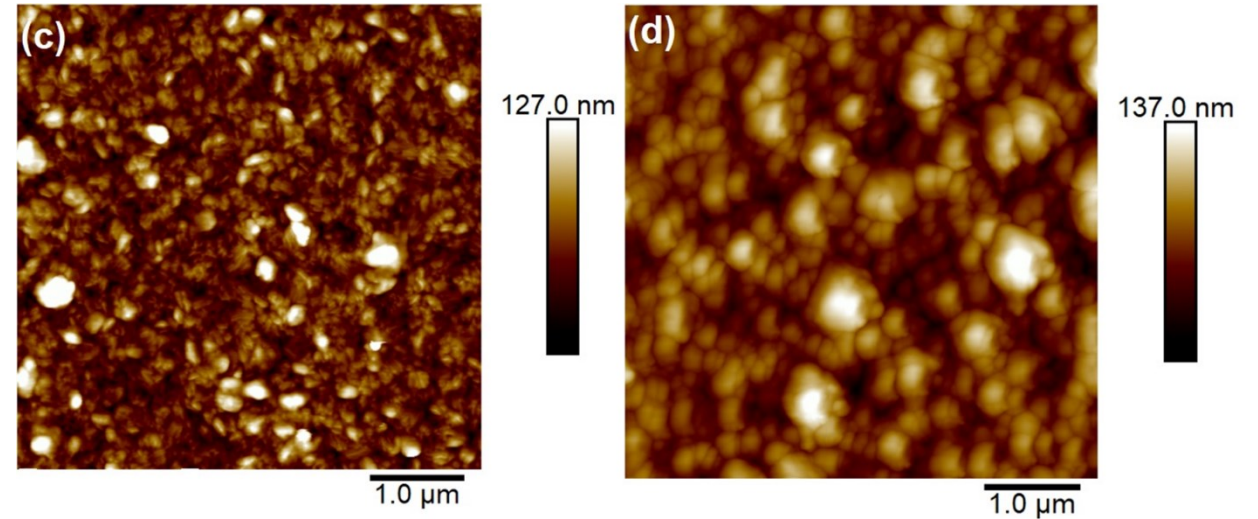
Chronoamperometry of sample CuFeO_ECWR_x4x , annealed at 550°C in argon, measured at -0.6 V vs. Ag/AgCl , 1 mol/l NaOH

Plasma diagnostics by RF planar probe during the deposition process

Deposition of CuFeO_2 with Cu and Fe target in $\text{Ar}+\text{O}_2$ gas mixture (A. Písaříková, et. al. to be published)

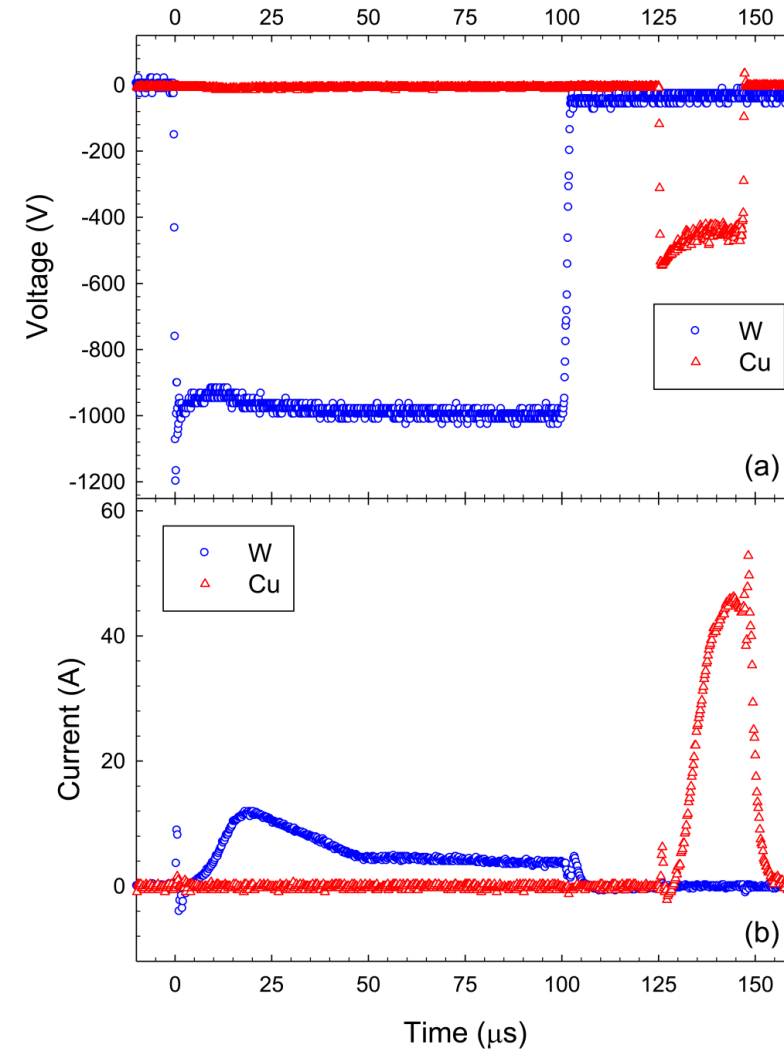
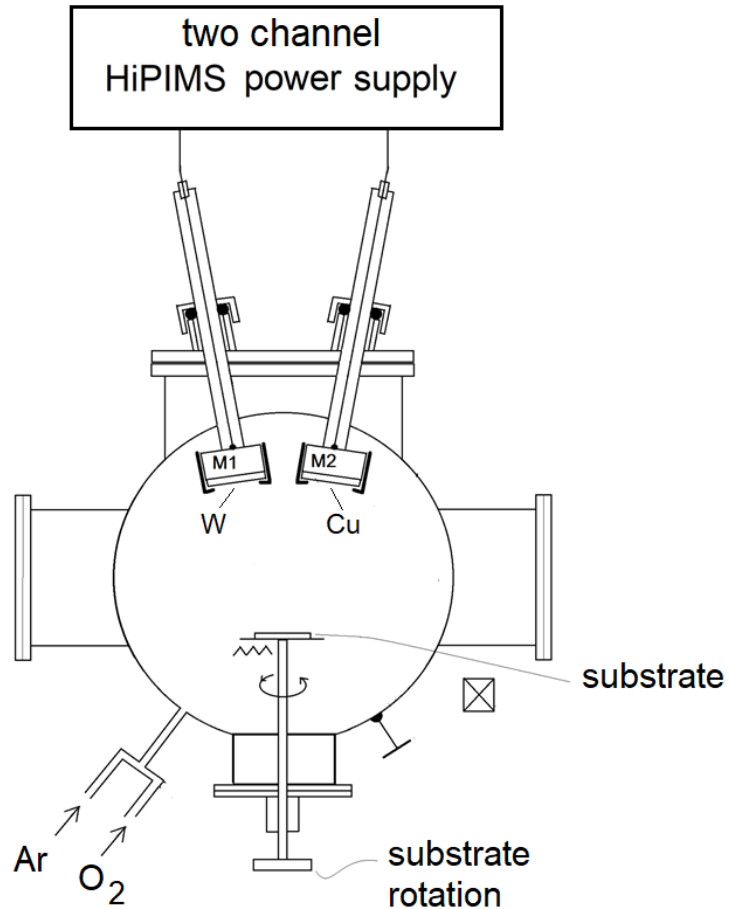


X-ray diffractograms of as-deposited (black) and annealed (red) samples deposited by r-HiPIMS+ECWR on FTO glass



Surface morphology of CuFeO_2 of as-deposited and annealed samples. (c), (d) as-deposited and annealed films of CuFeO_2 prepared by r-HiPIMS + ECWR, respectively.

Deposition of tungsten copper oxide (WCu_xO_y) films by reactive high power impulse magnetron co-sputtering (W and Cu targets in $\text{Ar}+\text{O}_2$ gas mixture).



Deposition of tungsten copper oxide (WCu_xO_y) films by reactive high power impulse magnetron co-sputtering (W and Cu targets in $\text{Ar}+\text{O}_2$ gas mixture).

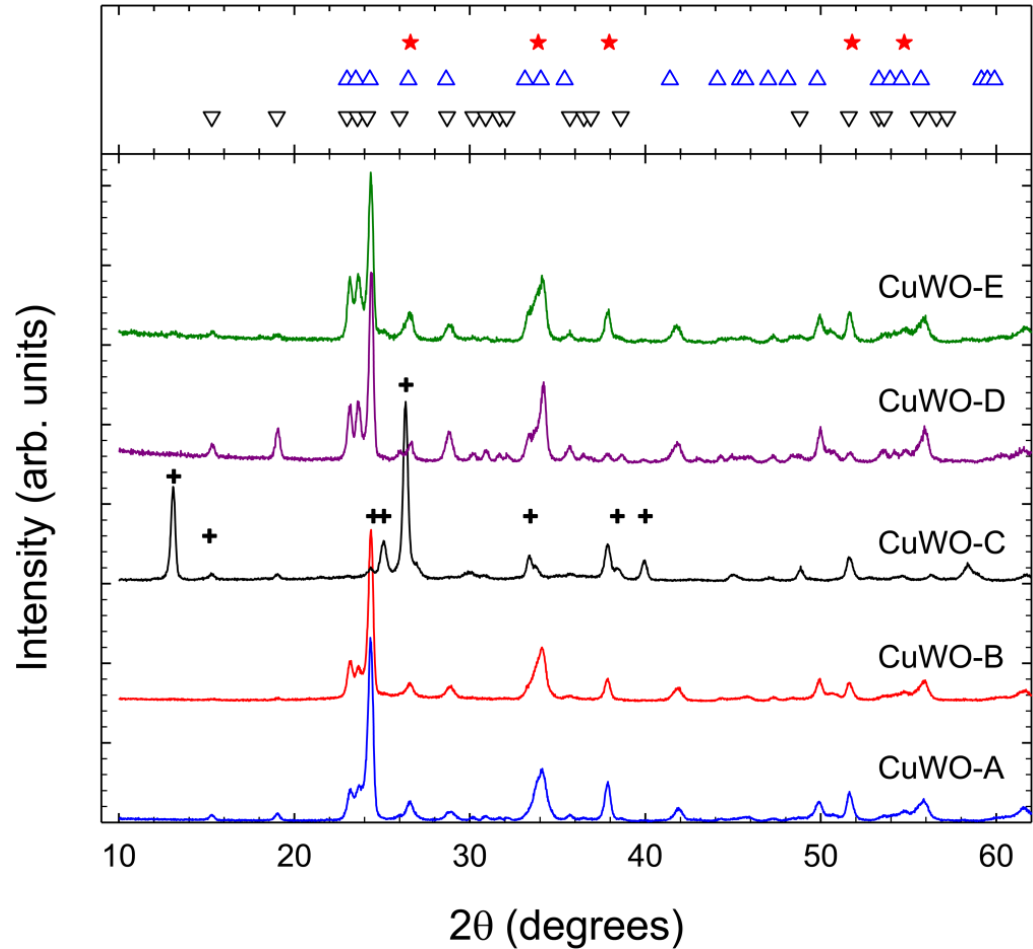
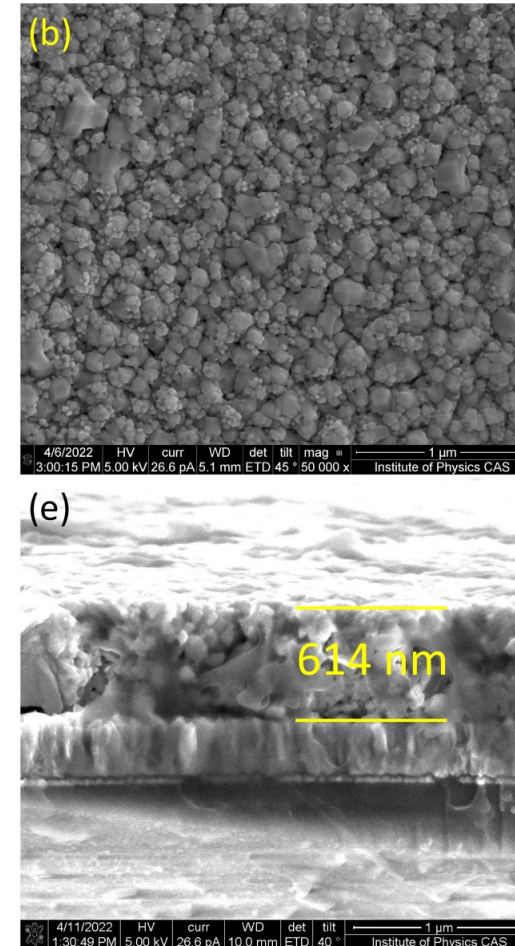
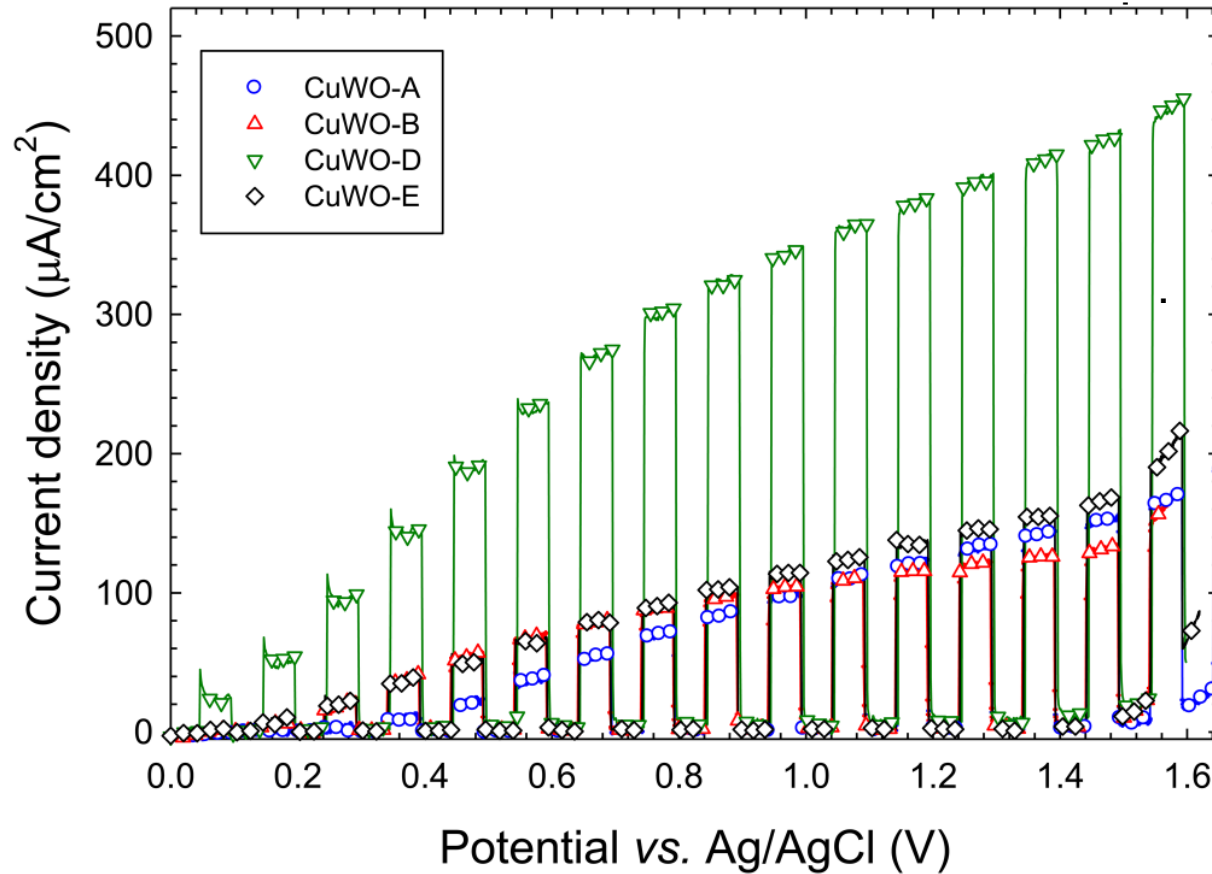


TABLE. Main crystallographic phases of annealed films on microscope glass (MG) and FTO-coated glass as obtained from the GIXRD measurements.

Sample	MG	FTO
CuWO-A	$\text{Na}_2\text{W}_2\text{O}_7$	$\text{WO}_3 + \text{CuWO}_4$ (10%)
CuWO-B	$\text{Na}_2\text{W}_4\text{O}_{13} + \text{Na}_2\text{W}_2\text{O}_7$ (15%)	WO_3
CuWO-C	CuWO_4	Cu_2WO_4
CuWO-D	$\text{WO}_3 + \text{CuWO}_4$ (50%)	$\text{WO}_3 + \text{CuWO}_4$ (25%)
CuWO-E	$\text{Na}_2\text{W}_2\text{O}_7 + \text{Na}_2\text{W}_4\text{O}_{13}$ (46%) + CuWO_4 (8%)	$\text{WO}_3 + \text{CuWO}_4$ (10%)

GIXRD diffractogram of annealed Cu_xWO_y films deposited by HiPIMS on FTO-coated glass substrates. Reflections from the assumed monoclinic Cu_2WO_4 (+), monoclinic WO_3 (Δ), CuWO_4 (∇), and FTO (*) are indicated.

Deposition of tungsten copper oxide (WCu_xO_y) films by reactive high power impulse magnetron co-sputtering (W and Cu targets in $\text{Ar}+\text{O}_2$ gas mixture).



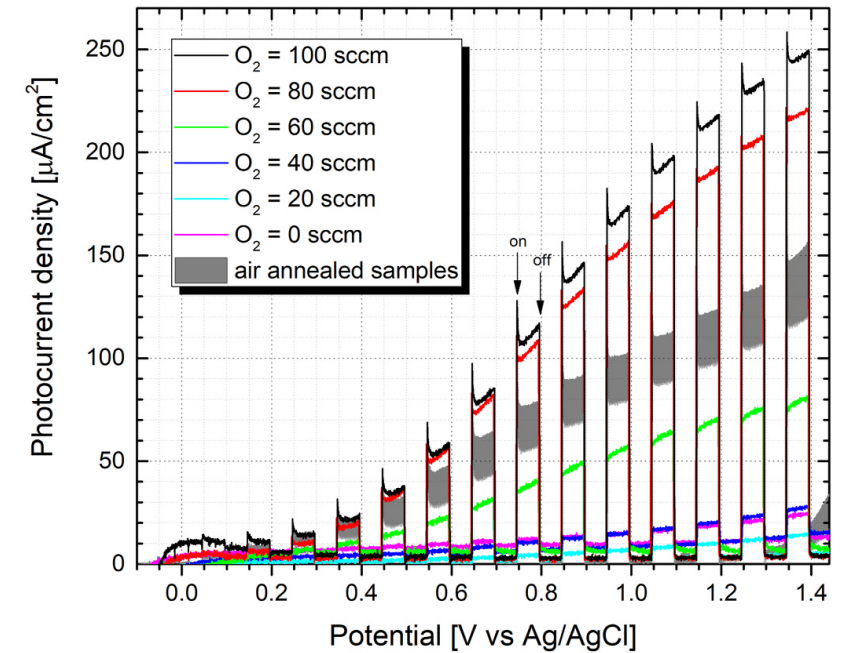
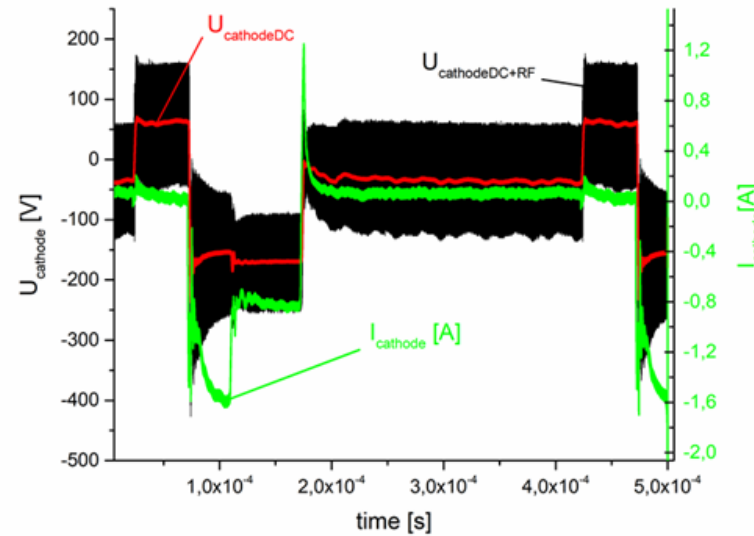
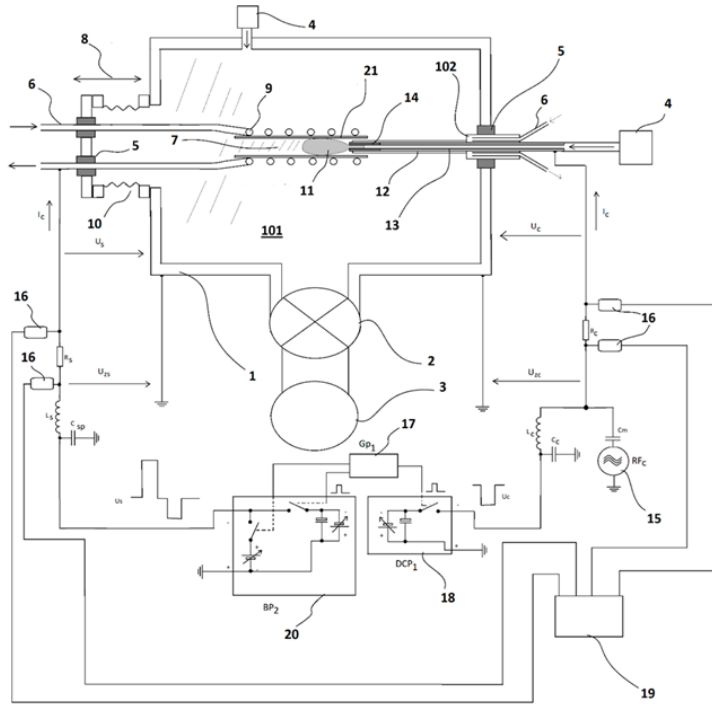
SEM
CuWO-D (FTO)
 $\text{WO}_3 + \text{CuWO}_4$ 25%

Current density of annealed Cu_xWO_y on FTO) as a function of applied voltage under simulated solar light irradiation with an intensity of 0.62 sun. Scan rate 10 mV/s, electrolyte 0.1 mol/l Na_2SO_4 , periodically illuminated 5 s dark/5 s light.

VP5 international patent (deposition of catalytic films in tubes)

Team of VP5 developed new hollow cathode pulsed deposition plasma jet method for deposition of thin films

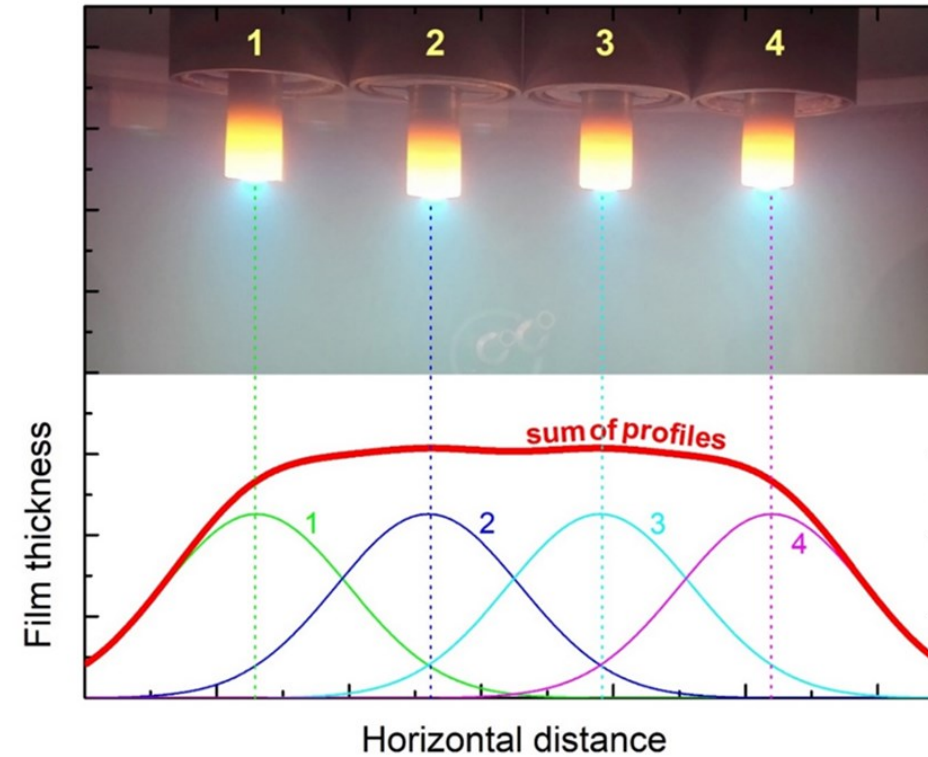
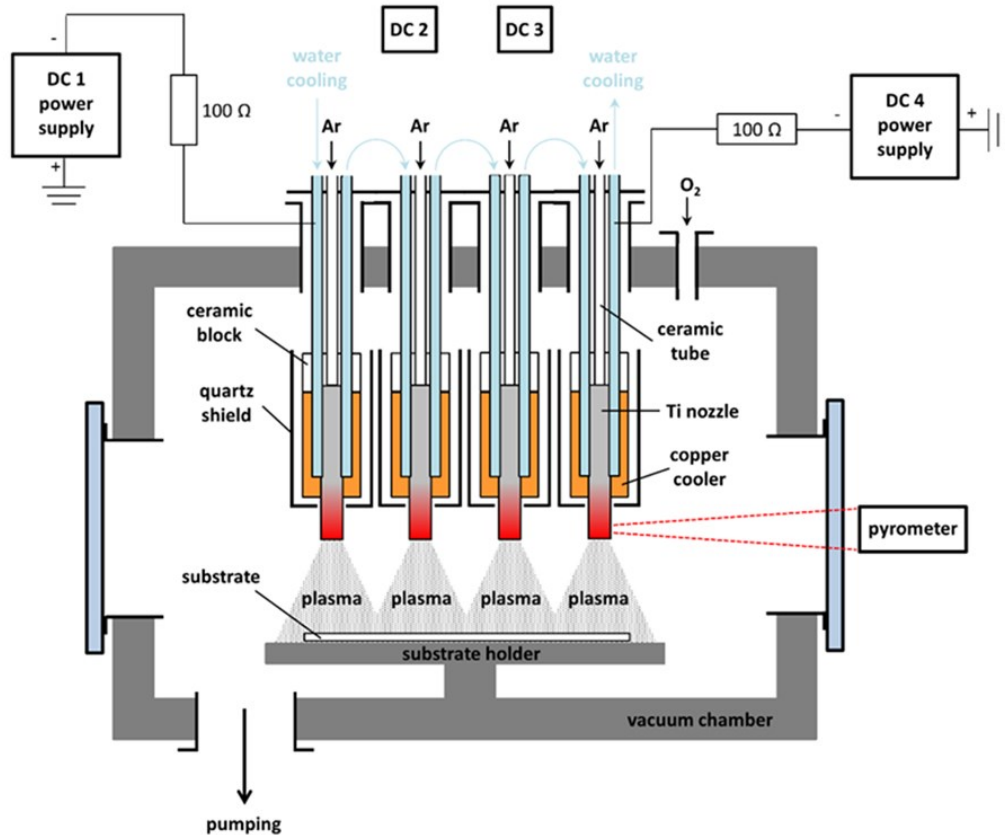
Z. Hubička, M. Čada, P. Kšířová, M. Klinger, A method of generating low temperature plasma, a method of coating the inner surface of hollow electrically conductive or ferromagnetic tubes and the equipment for doing this, PV-2018-206307842, PCT/CZ2019/050019, WO 2019/210891 A1, EU patent EP3788181A1



2) J.Olejníček, A.Hrubantová, L.Volfová, M.Dvořáková, M.Kohout, D.Tvarog, O.Gedeon, H.Wulff, R.Hippler, Z.Hubička, WO_3 and WO_{3-x} thin films prepared by DC hollow cathode discharge, Vacuum 195 (2022), 110679.

Cooperation between IQ structures, s.r.o. - FZU AVČR, v.v.i. - thin film optical security elements for bank notes

High rate deposition of homogeneous oxide semiconductor films by pulse multi-nozzle system of hot hollow cathodes
- the system was already sold as a prototype to IQS group, s.r.o. as a deposition source for implementation in large industrial roll to roll coater



Reactive pulse sputtering system for sulphides and selenides was installed and finished

- polycrystalline LuS_2 semiconductor films were deposited for RP3
- MoS_2 semiconductor thin films were deposited for photonic applications with HiLASE
- the bilayer structure WO_3/WS_2 is being prepared for sensory application



SOLID21

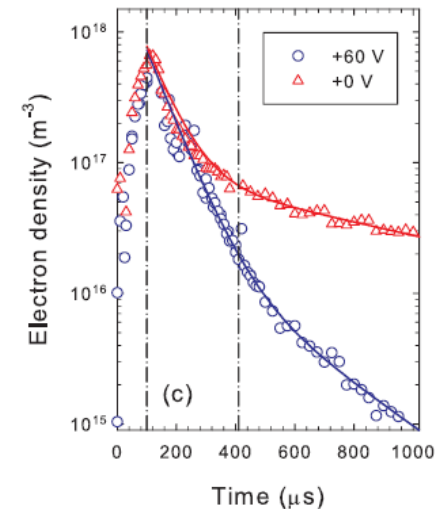
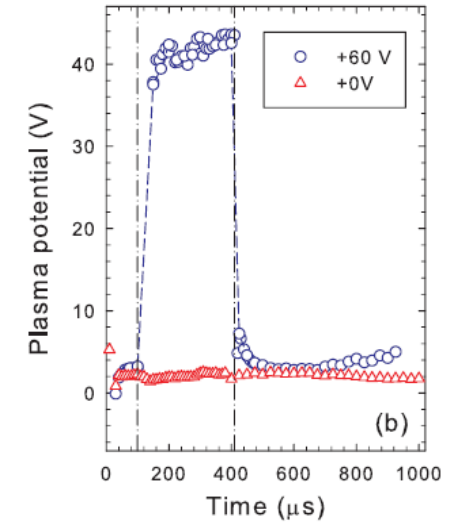
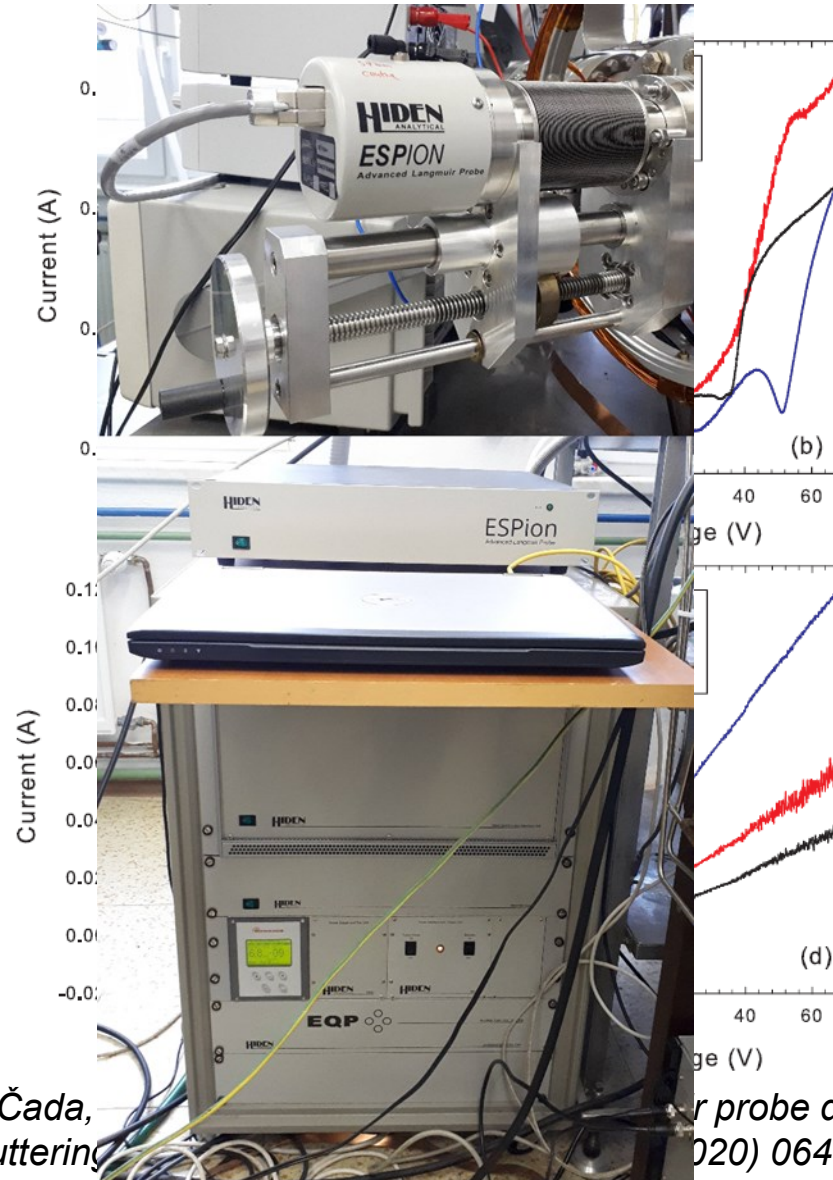
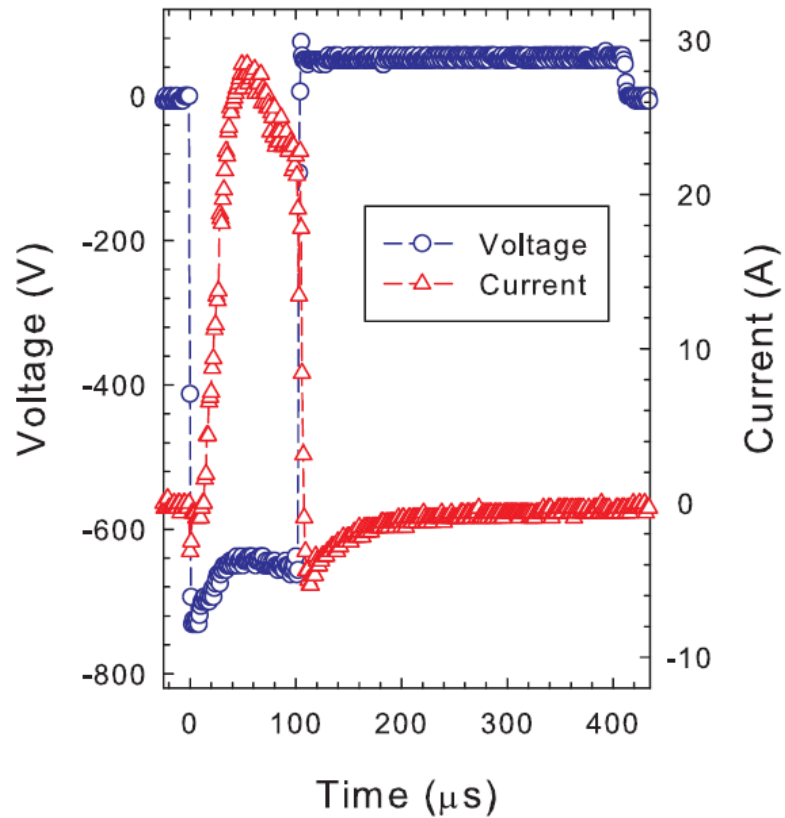
Research program 2

RP leader
Martin Čada

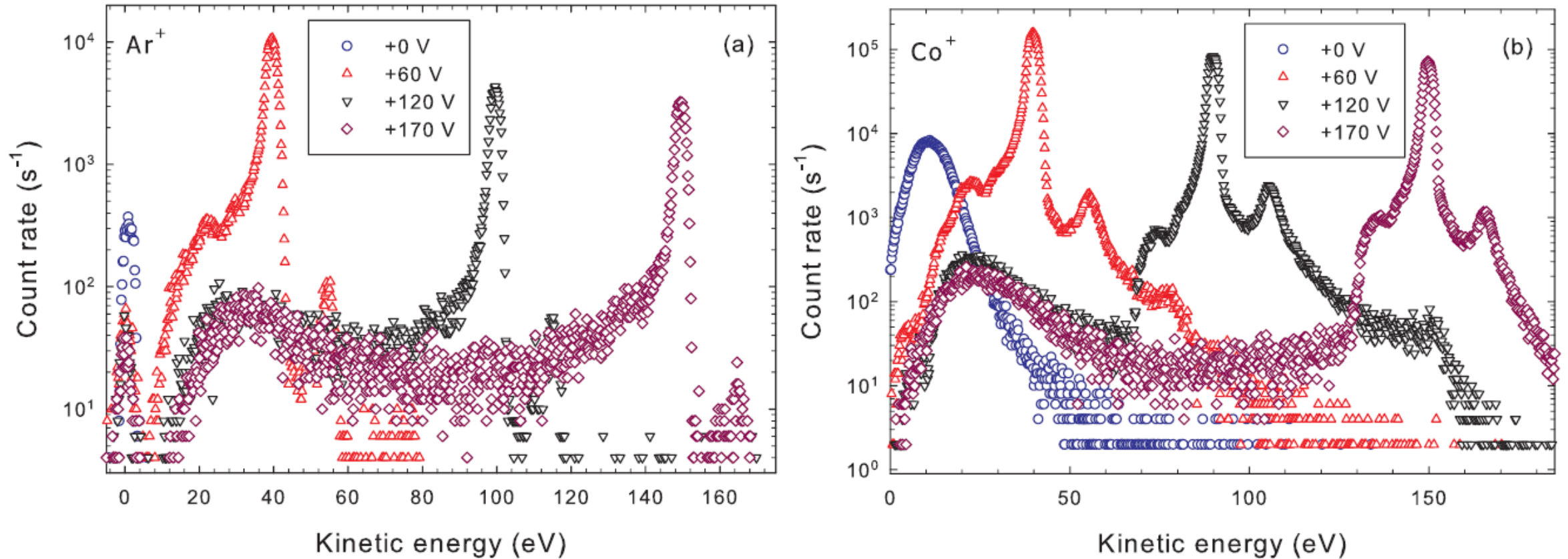
VP5 - plasma diagnostic of reactive r-HiPIMS and bipolar r-HiPIMS plasma

bipolar HiPIMS

- time resolved Langmuir probe measurements of bipolar HiPIMS plasma during positive pulse



-ion mass spectrometry with energetic resolution for different values of positive pulse



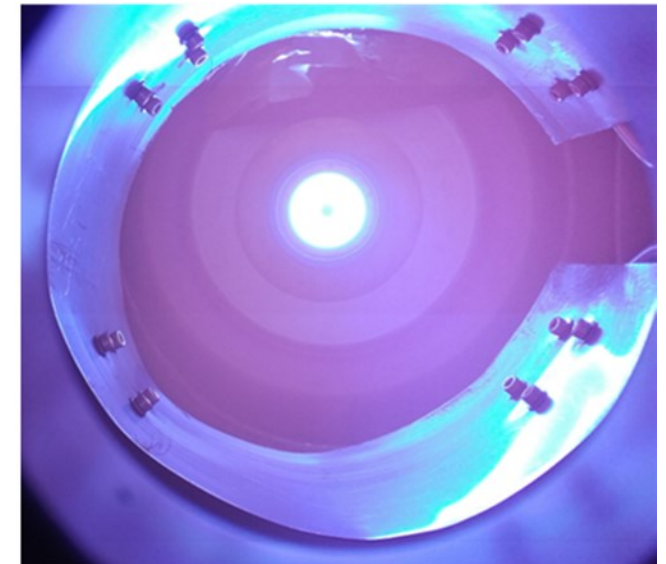
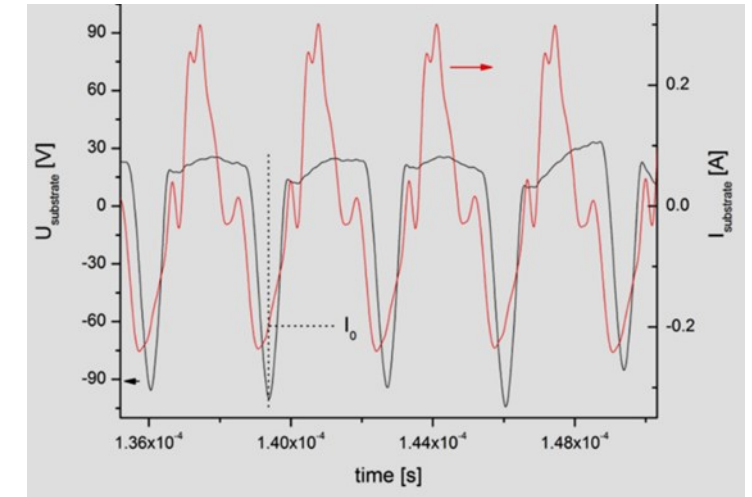
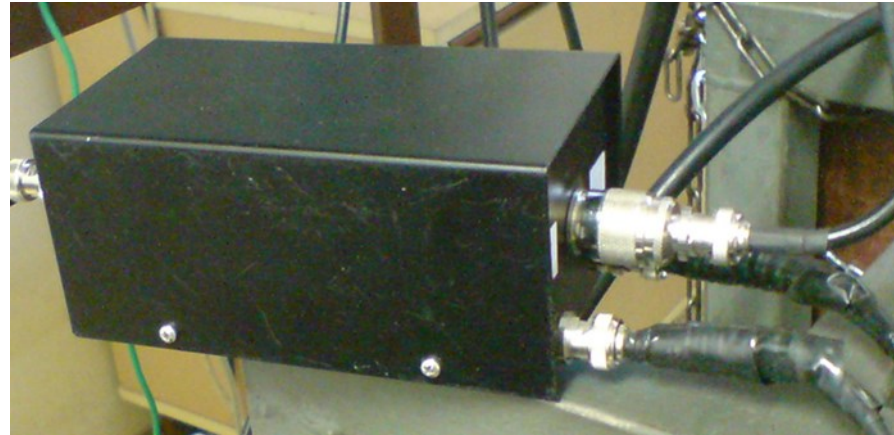
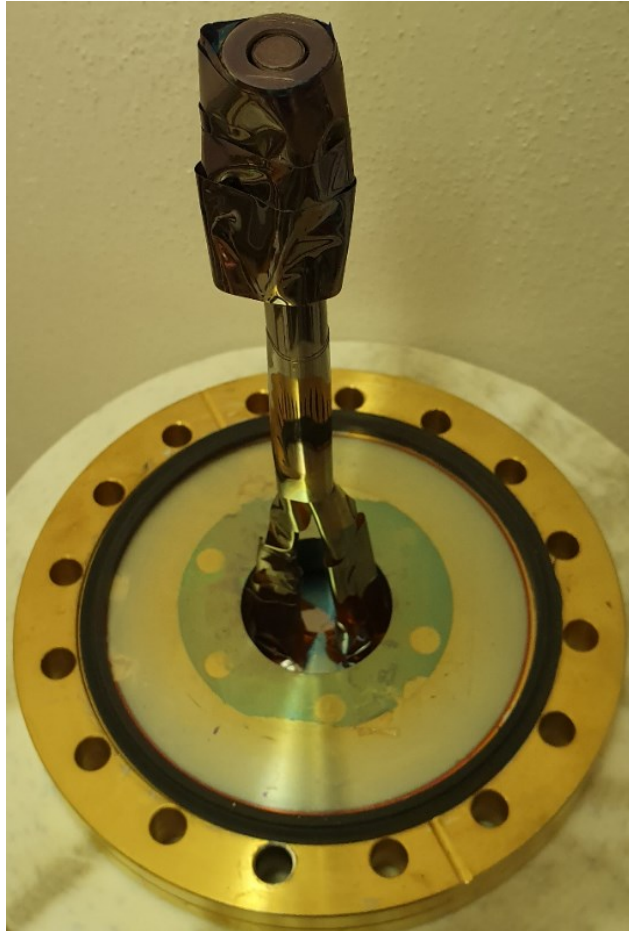
FZU

Fyzikální ústav
Akademie věd
České republiky

R. Hippler, M. Čada, Z. Hubička, Time-resolved Langmuir probe diagnostics of a bipolar high power impulse magnetron sputtering discharge, *Appl. Phys. Lett.* 116 (2020) 064101.

HiPIMS or HiPIMS+ECWR with dual magnetron for alloy and multicomponent thin films

RF planar probe



Plasma diagnostics by RF planar probe during the deposition process

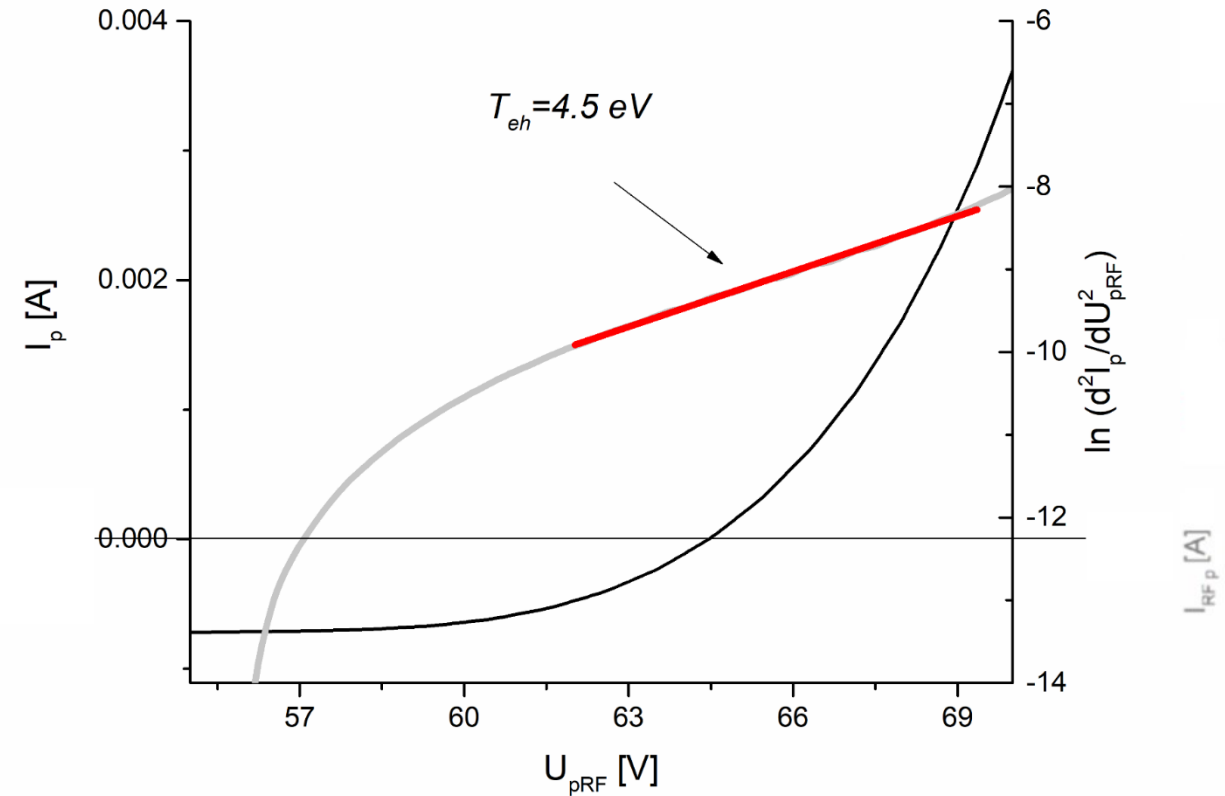
$f_p \ll f_{ion}$ we can use analytical model

$$i_{ionflux} = e \times n_i \times \sqrt{\frac{k_B T_e}{M_i}} \times 0.6$$

$$I_p(t) = I_{RFp}(t) - C_p(U_{RFp}) \frac{dU_{RFp}}{dt}(t)$$

$$(1) \quad \frac{dU_{RFp}}{dt} > 0 \quad I_{RFp} = I_{SA}(U_{RFp}) = I_p(U_{RFp}) + C_p(U_{RFp}) \frac{dU_{RFpA}}{dt}(U_{RFp})$$

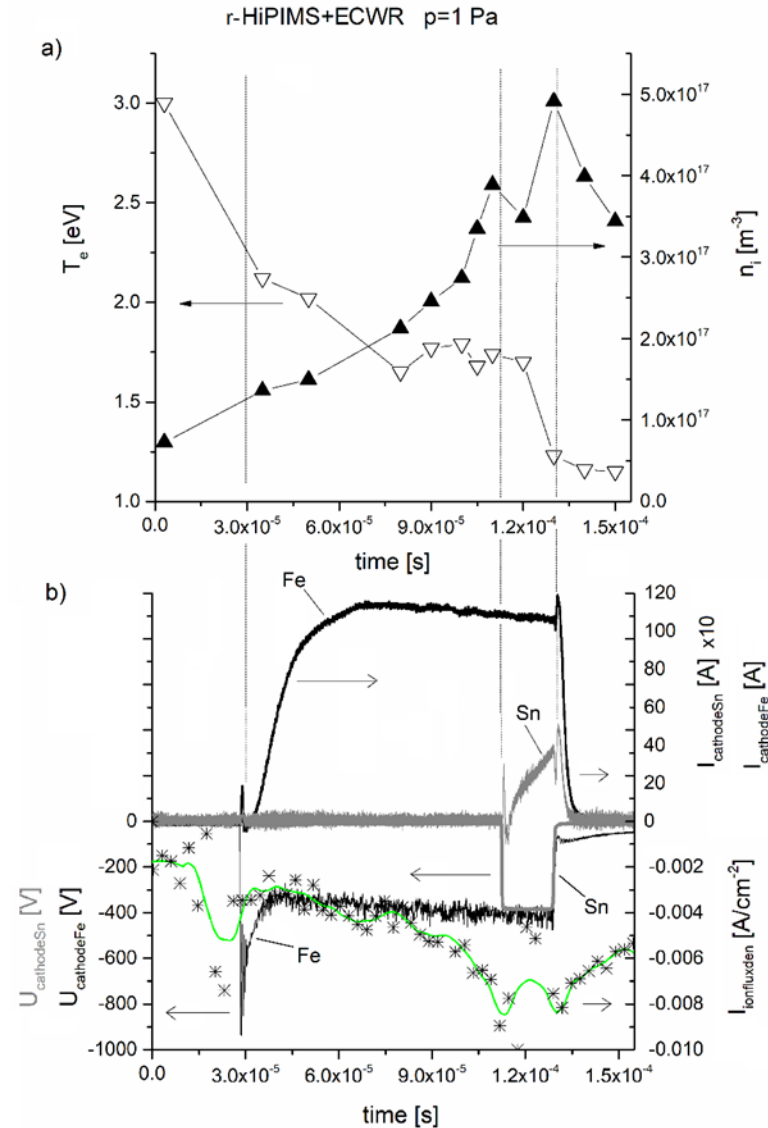
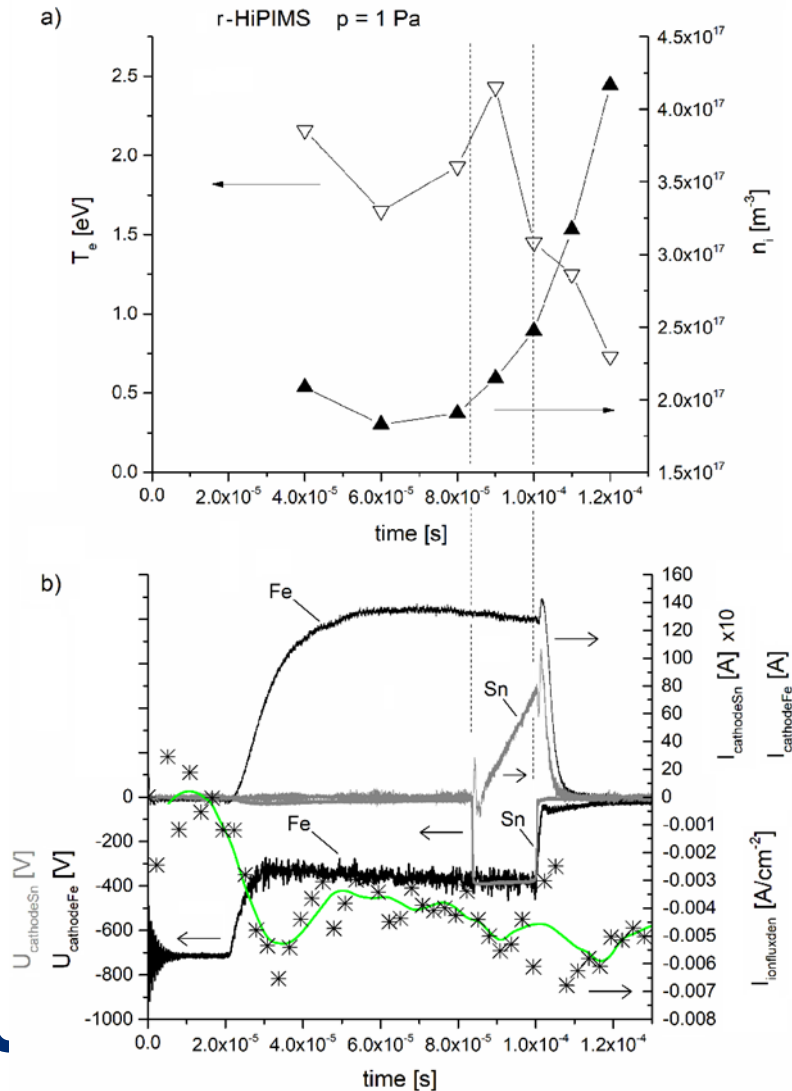
$$(2) \quad \frac{dU_{RFp}}{dt} < 0 \quad I_{RFp} = I_{SB}(U_{RFp}) = I_p(U_{RFp}) + C_p(U_{RFp}) \frac{dU_{RFpB}}{dt}(U_{RFp})$$



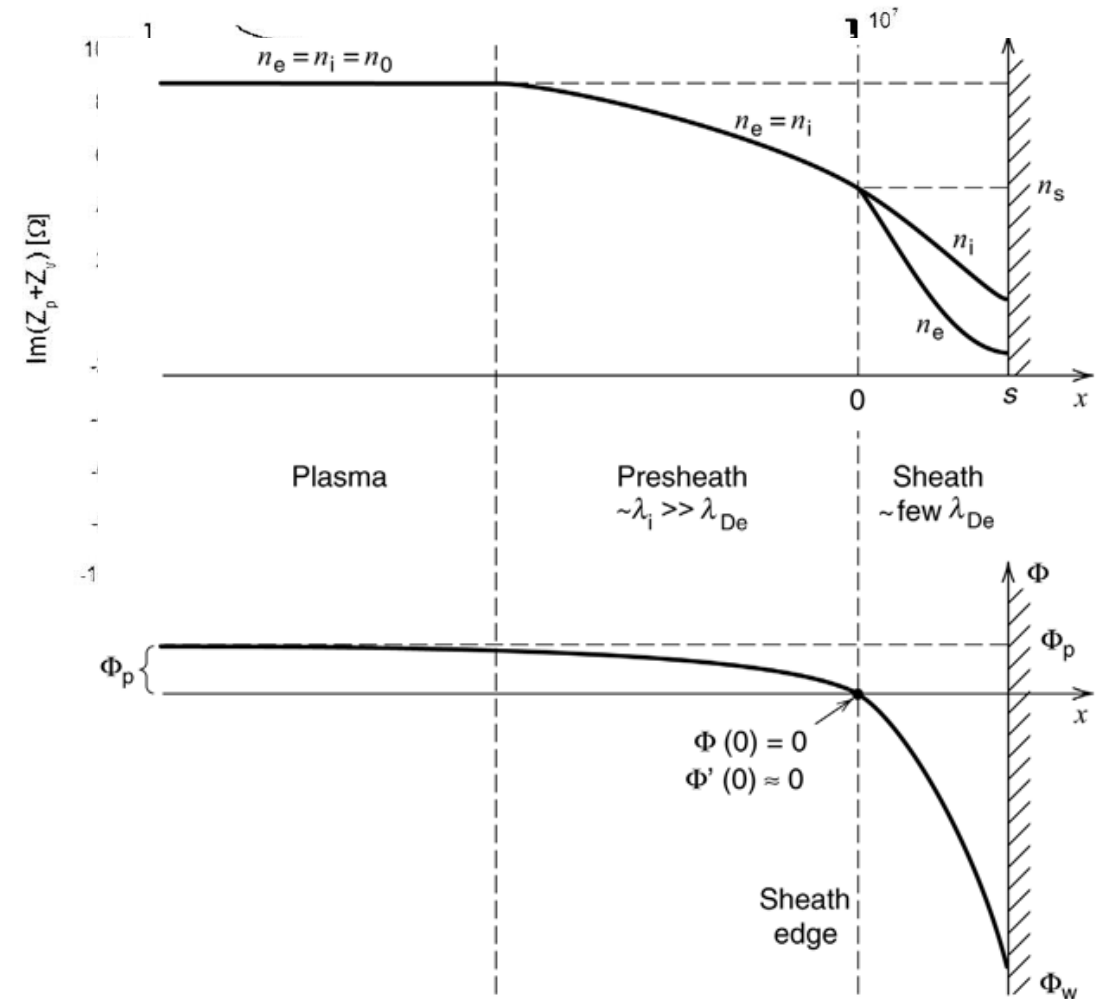
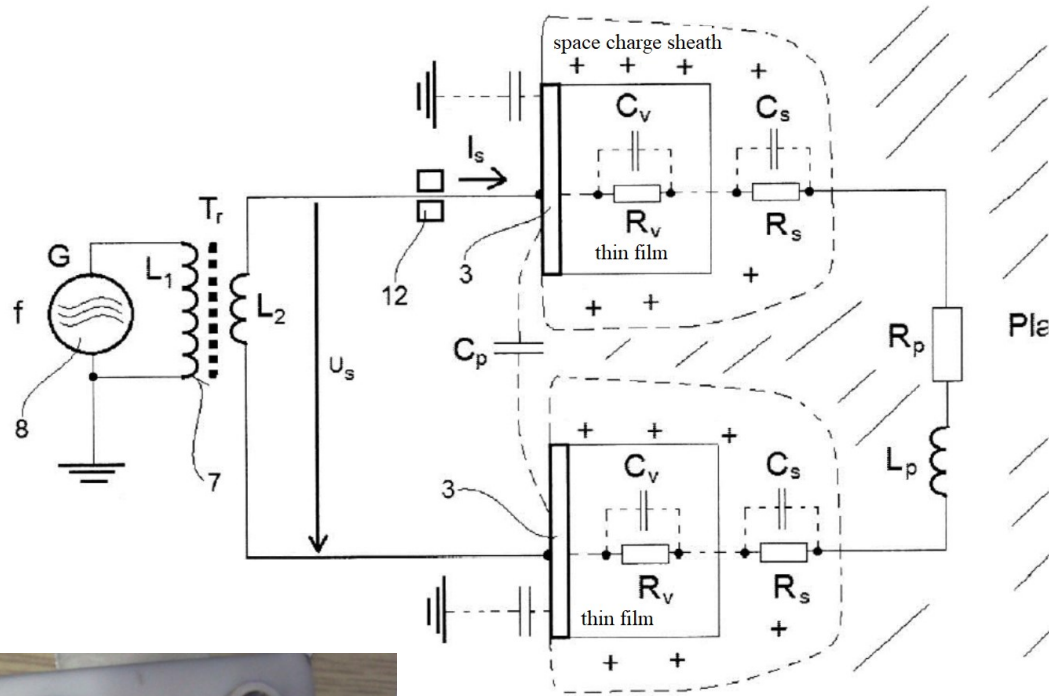
Sezemský, P.; Straňák, V.; Kratochvíl, J.; Čada, M.; Hippler, R.; Hrabovský, M.; Hubicka, Z. Modified high frequency probe approach for diagnostics of highly reactive plasma. *Plasma Sources Sci. Technol.* **2019**, *28*, 115009, doi:10.1088/1361-6595/ab506c.

RF probe diagnostics at plasma deposition of $\text{Fe}_2\text{O}_3\text{:Sn}$ semiconducting (n-type) thin films

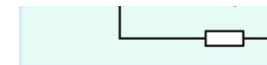
- plasma parameters measured by RF probe in r-HiPIMS and r-HiPIMS+ECWR during deposition



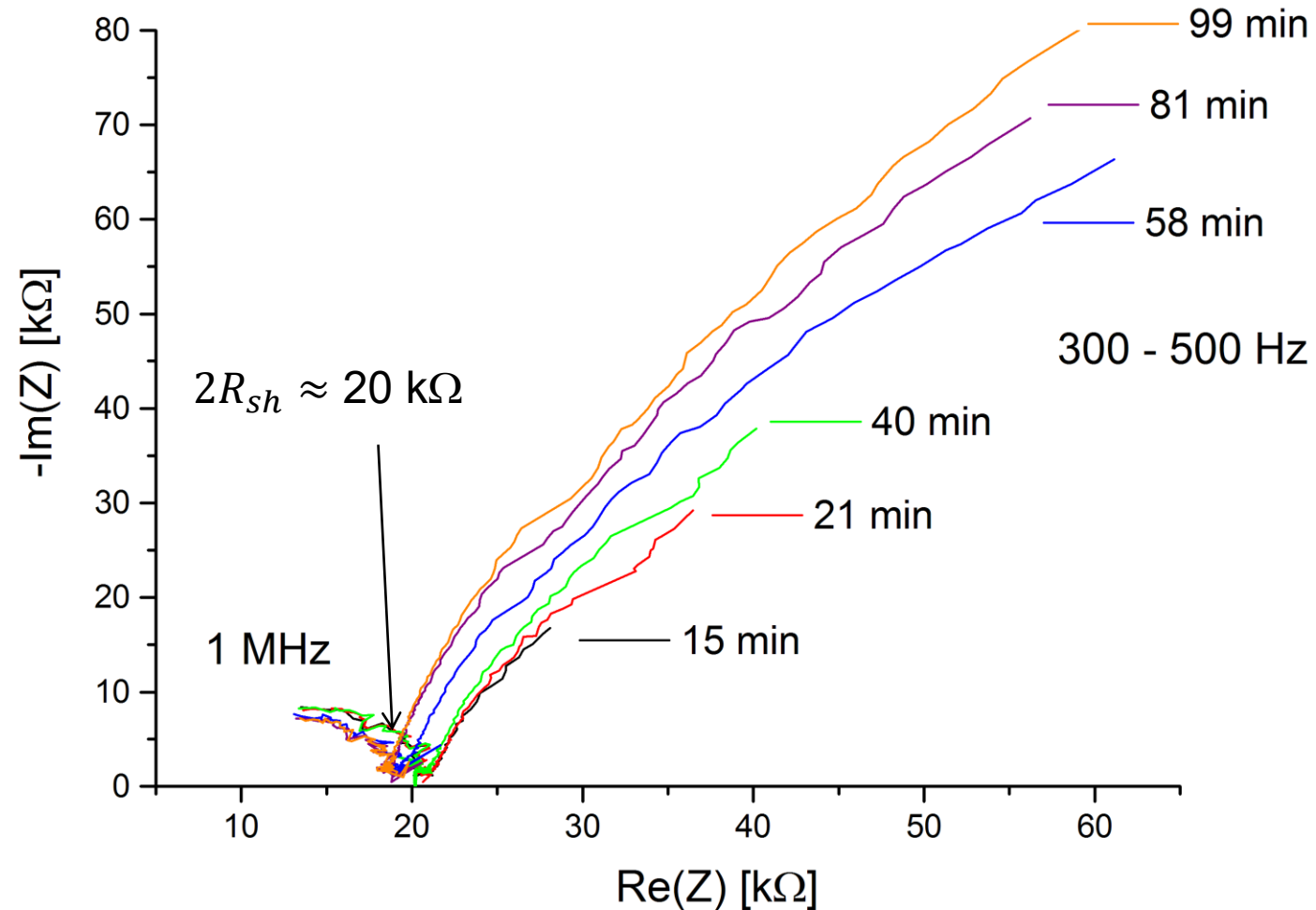
Impedance spectroscopy of system plasma-semiconductor film



Qualitative behavior of sheath and presheath in contact with a wall.

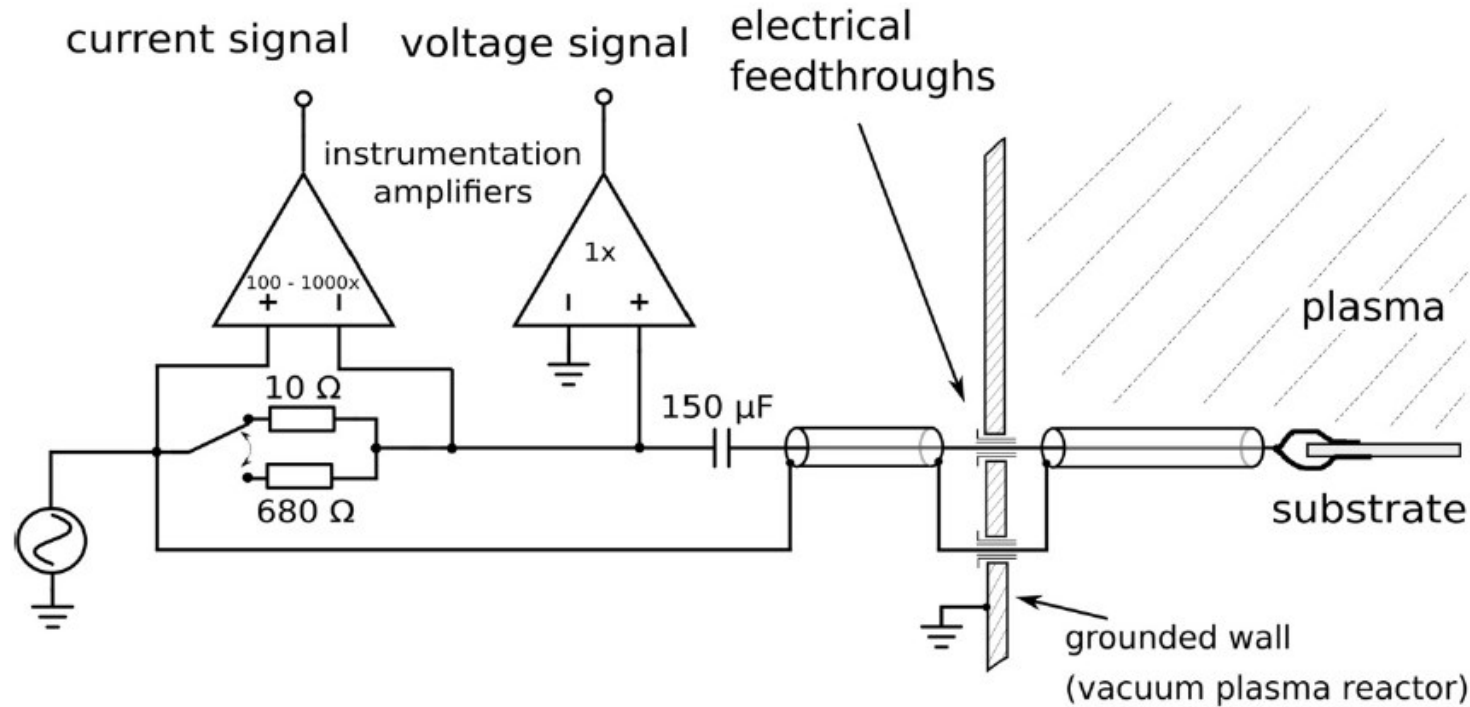


Measurement of impedance spectra during the deposition of TiO_2 by reactive sputtering process

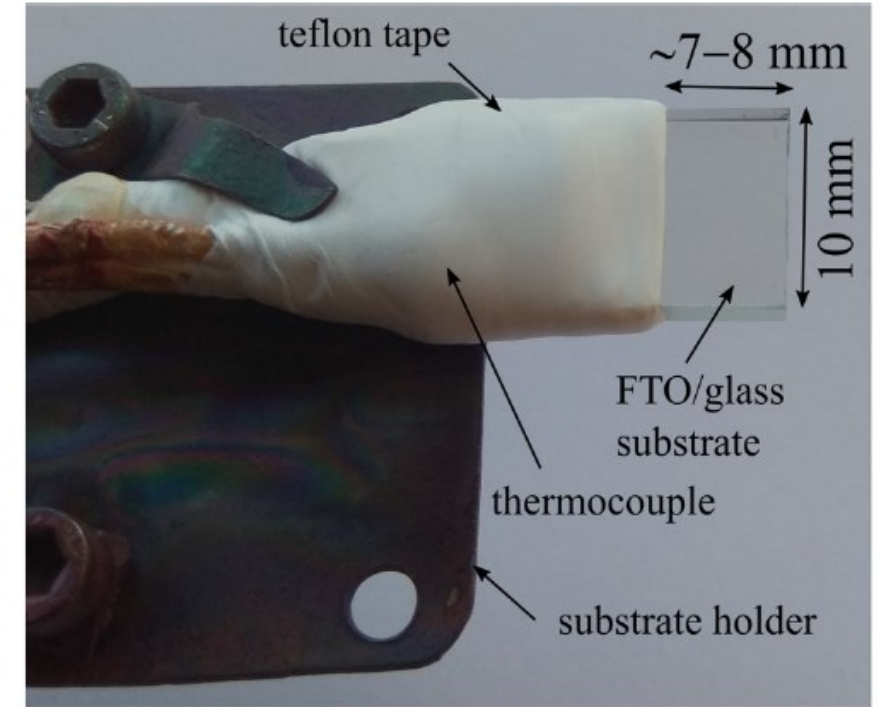


Each frequency dependence (300 values of frequencies equidistant in logarithmic scale) was measured 45 second

In-situ impedance spectroscopy of a plasma-semiconductor thin film system during reactive sputter deposition



(a)



(b)

FIG. 3. (a) Measuring circuit together with the connection to the probe/substrate. (b) Photo of the substrate and substrate holder prior to the deposition.

M. Zanáška, P. Kudrna, M. Čada, M. Tichý, and Z. Hubička, In-situ impedance spectroscopy of a plasmasemiconductor thin film system during reactive sputter deposition J. Appl. Phys. 126, 023301 (2019); doi: 10.1063/1.5102163.

J. Morozumi, T. Goya, T. Kuyama, K. Eriguchi, K. Urabe, In situ electrical monitoring of SiO_2/Si structures in low-temperature plasma using impedance spectroscopy, Japanese Journal of Applied Physics 62, SI1010 (2023).

In-situ impedance spectroscopy of a plasma-semiconductor thin film system during reactive sputter deposition

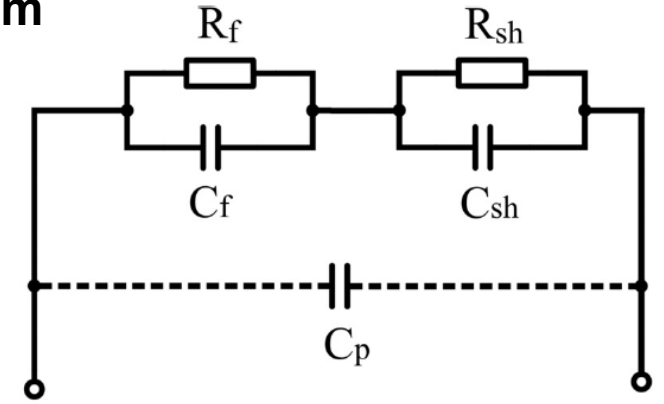
$$Z_f = Z - Z_s = Z - \frac{1}{1/R_s + i\omega C_s}$$

$$\frac{1}{Z_f} = \frac{1}{R_f} + i\omega C_f$$

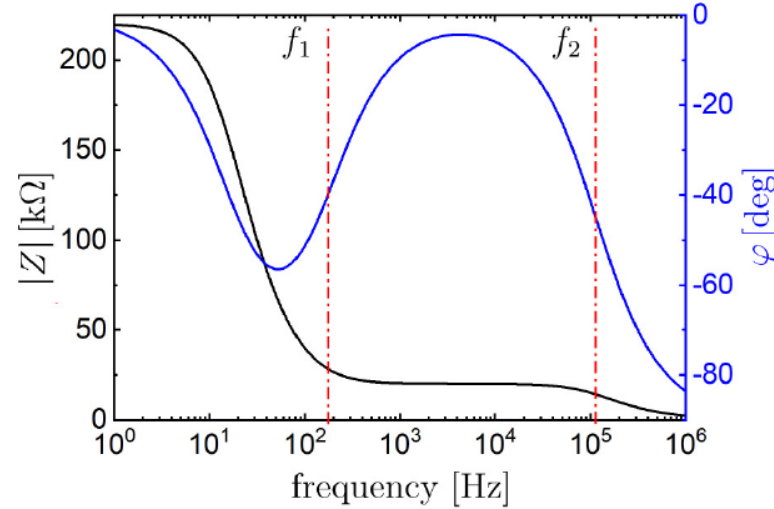
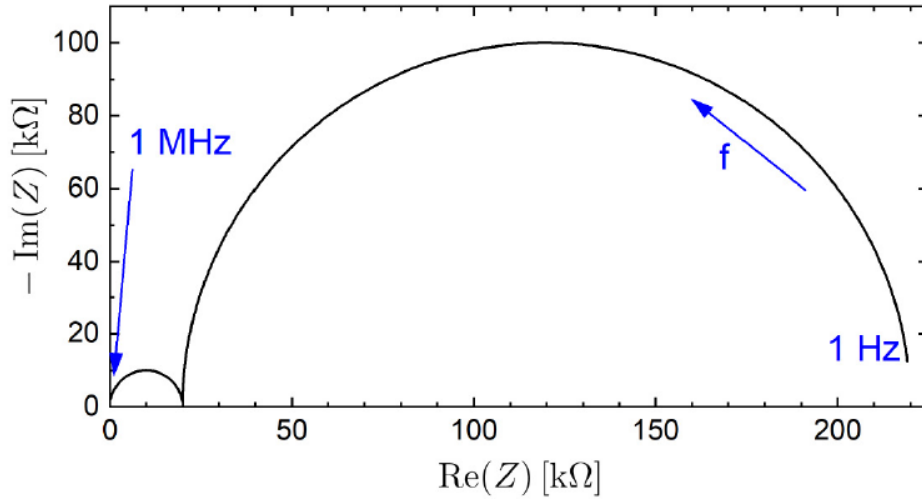
$$\varepsilon_r = \varepsilon'_r - i\varepsilon''_r = \varepsilon'_r - \frac{i\sigma}{\omega\varepsilon_0},$$

$$C_f = \frac{\varepsilon_0 \varepsilon'_r A}{d}, \quad R_f = \frac{d}{A\sigma},$$

$$\tan \delta = \frac{\varepsilon''_r}{\varepsilon'_r} = \frac{1}{\omega R_f C_f}.$$



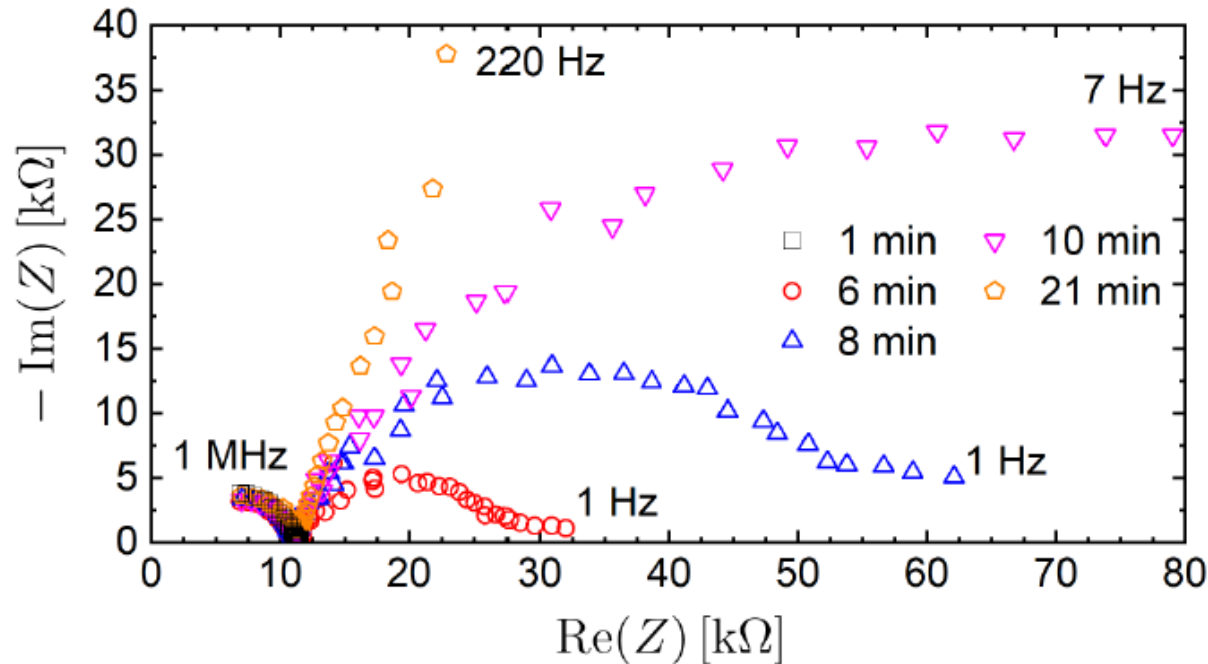
Simple equivalent circuit describing the impedance of the deposited thin film and the surrounding plasma sheath together with the parasitic capacitance C_p . R_s and C_s represent the sheath, R_f and C_f represent the deposited film.



(a) Nyquist plot and (b) Bode plot of the equivalent circuit depicted in Fig. 1, in the range from 1 Hz to 1 MHz for parameters: $R_s = 20 \text{ k}\Omega$, $C_s = 30 \text{ pF}$, $C_p = 40 \text{ pF}$, $R_f = 200 \text{ k}\Omega$, and $C_f = 50 \text{ nF}$. At these conditions, the effect of the parasitic capacitance is almost identical to the sheath capacitance, i.e., with changed parameters C_s and C_p such that $C_s + C_p = 70 \text{ pF}$, the difference in the spectrum is negligible. Note that the y axis in the Nyquist plot represents the negative imaginary part of the impedance.

In-situ impedance spectroscopy of a plasma-semiconductor thin film system during reactive sputter deposition

Results of time evolution of impedance spectra of Fe_2O_3 thin films during the growth process



Nyquist plot of the impedance during the deposition of Fe_2O_3 (#1). The effect of the parasitic capacitance and capacitance of the blocking capacitor has been subtracted. For clarity, we show only the spectra from the first 21 min of the deposition.

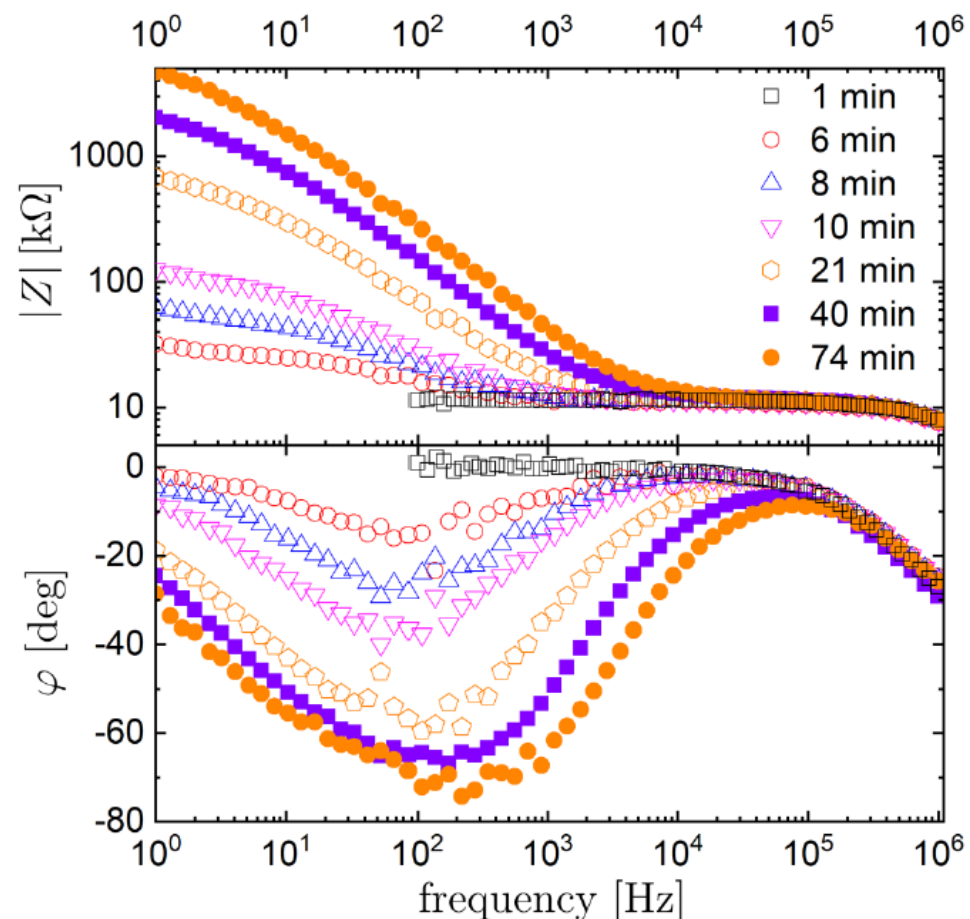


FZU

Fyzikální ústav
Akademie věd
České republiky

In-situ impedance spectroscopy of a plasma-semiconductor thin film system during reactive sputter deposition

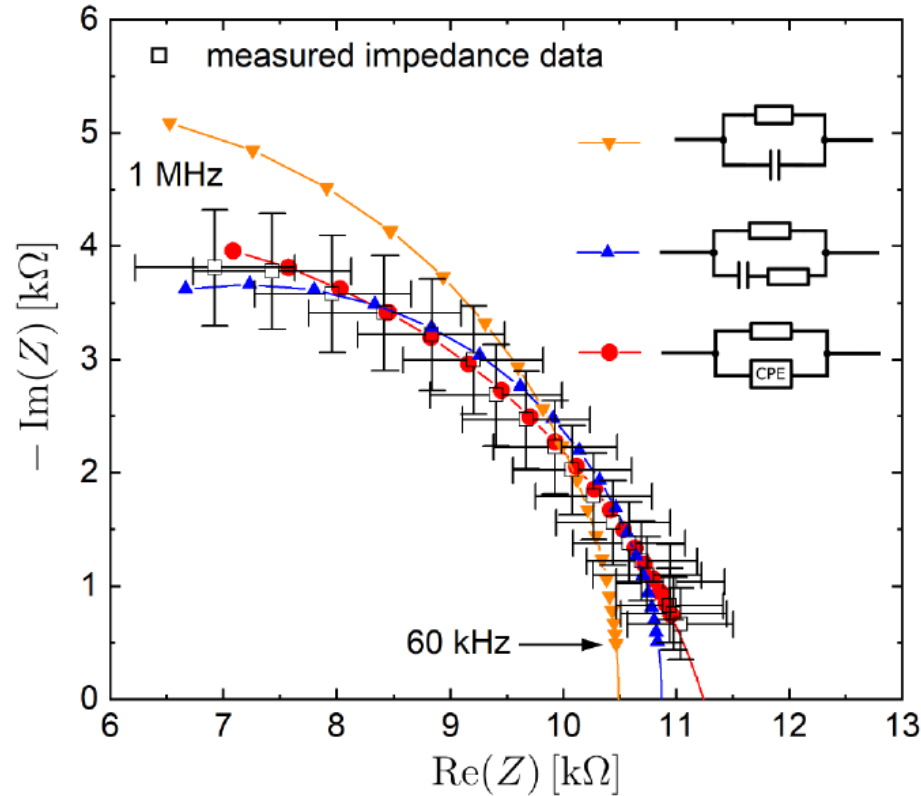
Results of time evolution of impedance spectra of Fe_2O_3 thin films during the growth process



Bode plot of impedance spectra measured during the deposition of the Fe_2O_3 film (#1).

In-situ impedance spectroscopy of a plasma-semiconductor thin film system during reactive sputter deposition

Fitting of impedance spectra of Fe_2O_3 thin films with different circuits models



$$Z_{CPE} = Q^{-1} (i\omega)^{-n}$$

$$0 \leq n \leq 1$$

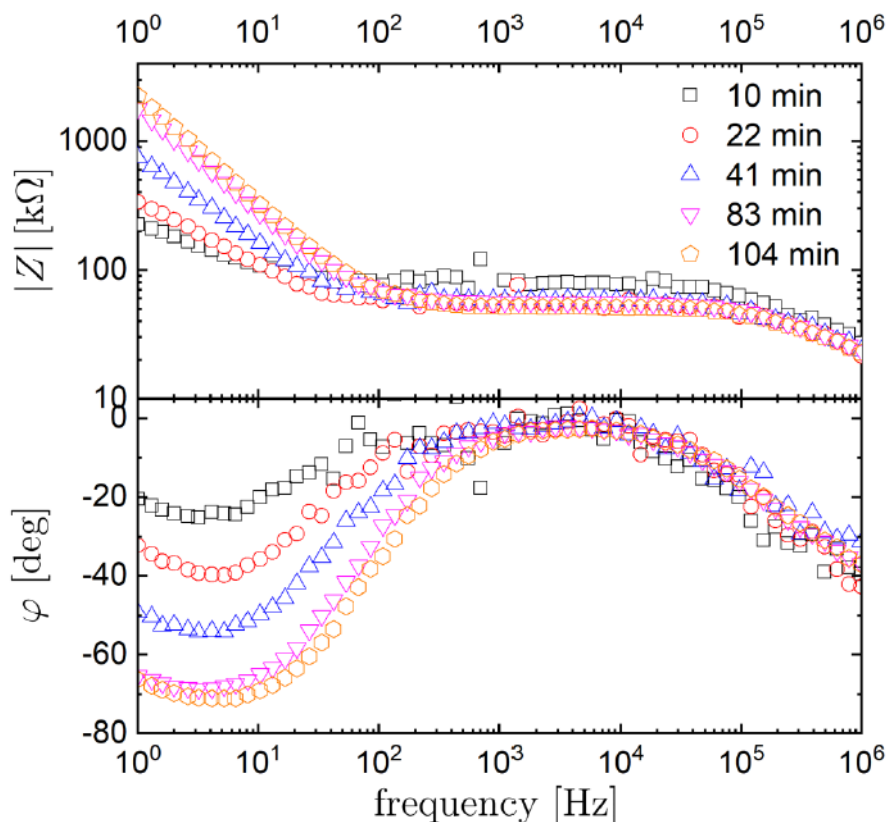
$$C = (QR^{1-n})^{1/n}$$

Nyquist plot of impedance spectrum after 1 min of the deposition of the Fe_2O_3 film (#1) and fits of three different models evaluated in the range 60 kHz–1 MHz. The points of the measured data and points at the fitted curves correspond to the same frequencies and indicate the frequency range of the fits. The fitted parameters of the third (red) model [and using Eq. (13)]: $R_s \approx 11.2 \text{ k}\Omega$, $C_s \approx 9 \text{ pF}$, $n \approx 0.8$.

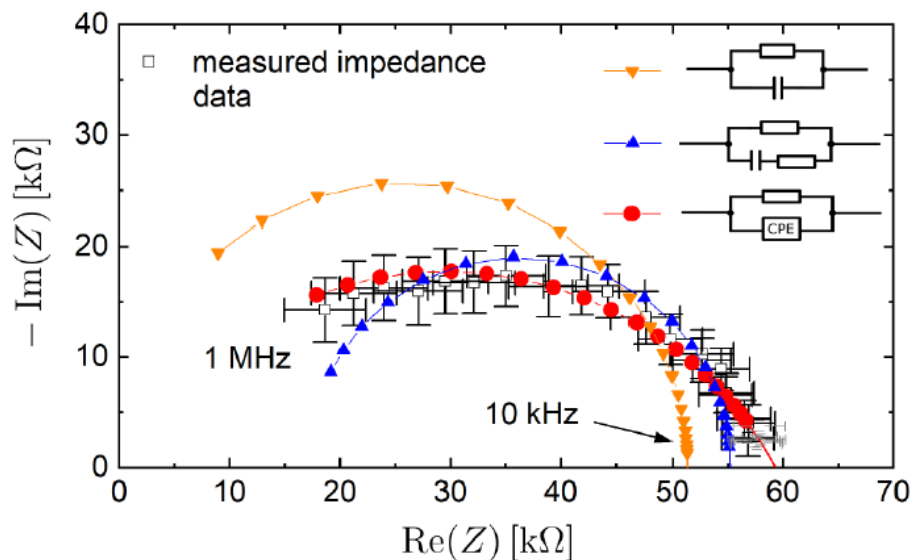


In-situ impedance spectroscopy of a plasma-semiconductor thin film system during reactive sputter deposition

Results of time evolution of impedance spectra of TiO_2 thin films during the growth process



Bode plot of impedance spectra measured during the deposition of the TiO_2 film (#3).



Nyquist plot of impedance spectrum during the deposition of TiO_2 (#3) and fits of three different models evaluated in the range 10 kHz–1 MHz. The points of the measured data and points at the fitted curves correspond to the same frequencies and indicate the frequency range of the fits. The fitted parameters of the third (red) model [and using Eq. (13)]: $R_s \approx 59.4 \text{ k}\Omega$, $C_s \approx 7 \text{ pF}$, $n \approx 0.7$.

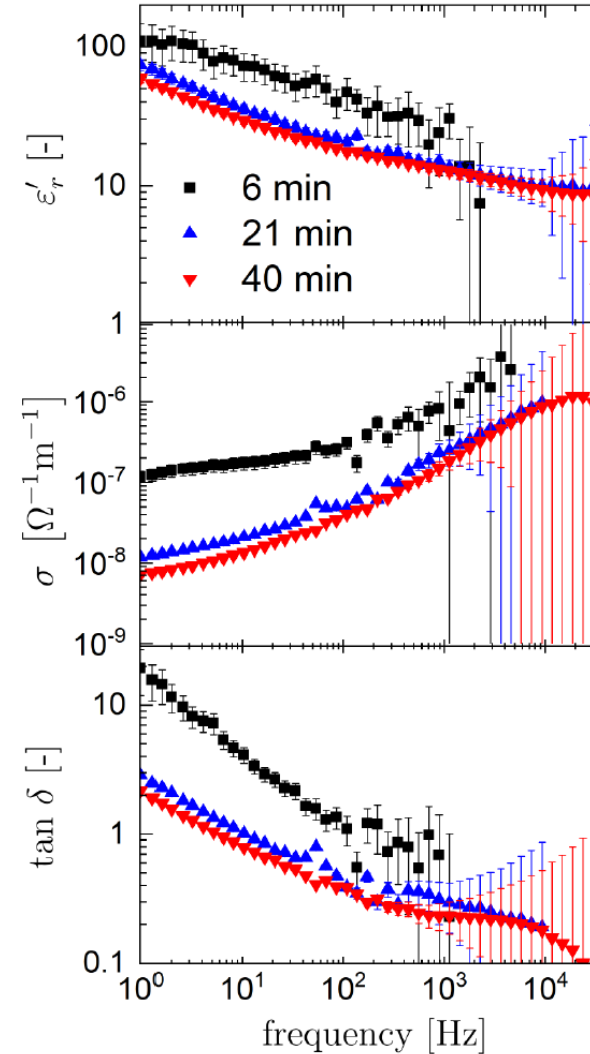


FZU

Ákademie věd
České republiky

Dielectric properties of the deposited films (Fe_2O_3)

thickness measured in time by QCM



Frequency dependence of the real part of the dielectric constant, conductivity, and dielectric loss of the deposited Fe_2O_3 (#1) film for three instants during the deposition. These data were retrieved from the impedance spectra shown in Figs. 4 and 5.

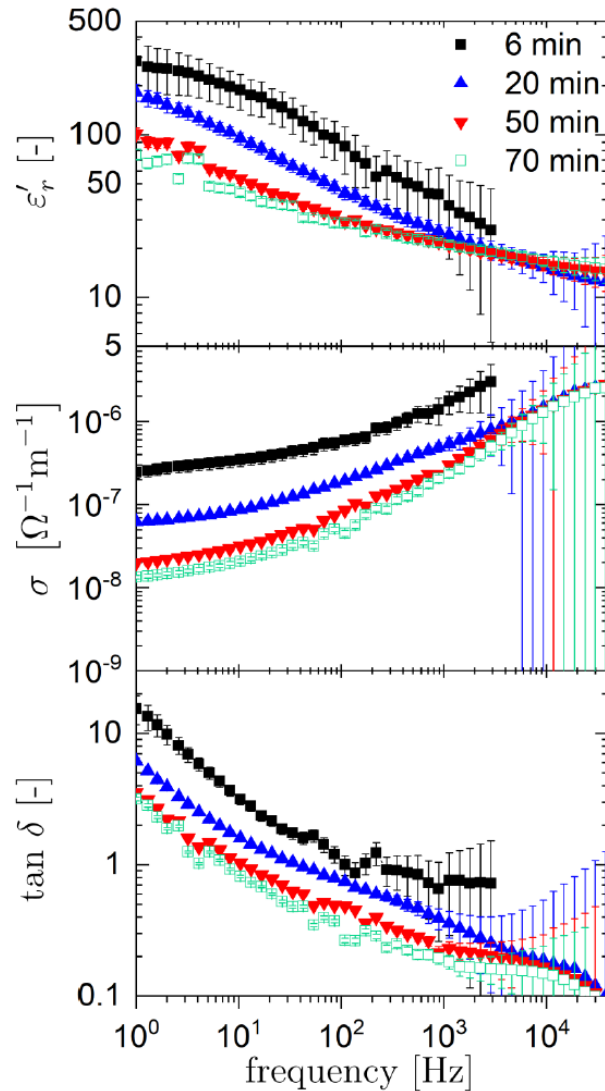


FZU

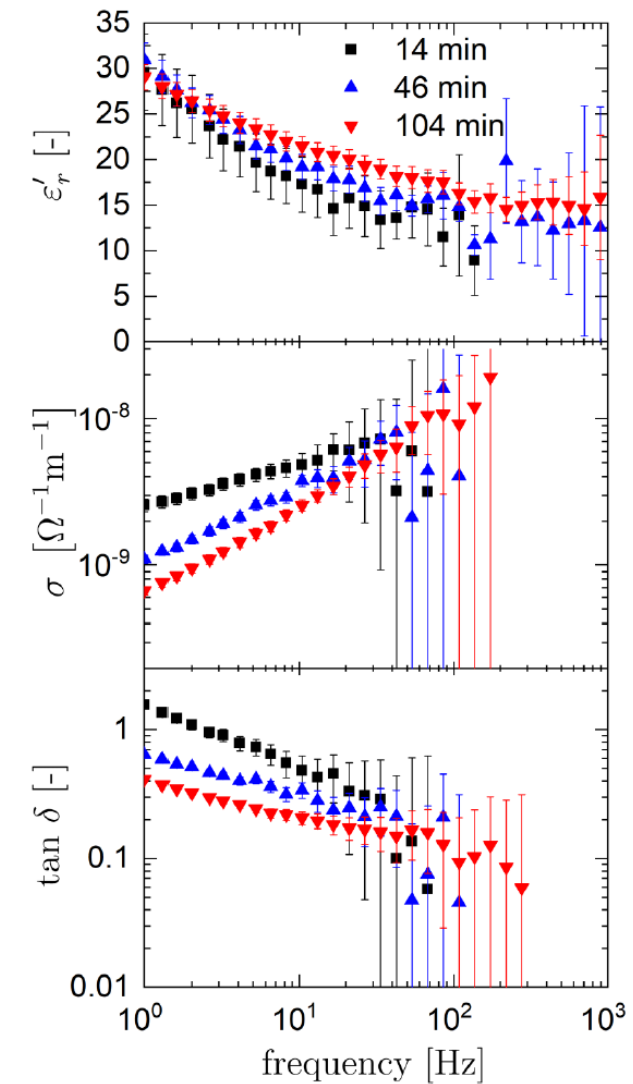
Fyzikální ústav
Akademie věd
České republiky

Dielectric properties of the deposited films (TiO₂)

thickness measured in time by QCM



Frequency dependence of the real part of the dielectric constant, conductivity, and dielectric loss of the deposited TiO₂ (#2) film for four instants during the deposition.



Frequency dependence of the real part of the dielectric constant, conductivity, and dielectric loss of the deposited TiO₂ film (#3) for three instants during the deposition.

RF probe + impedance spectroscopy + QCM ionmeter → international cooperation

- Dr. Daniel Lundin and professor Henrik Pedersen, University of Linköping Sweden
Plasma assisted CVD metal deposition - plasma diagnostics by RF probe
- Professor Tiberiu Minea, Paris-Sud University, France
plasma diagnostics of HiPIMS plasma by ionmeter and RF probe (Ph.D student Anna Kapran)
- Dr. Daniel Lundin Ionautics
RF probe and plasma impedance spectroscopy of reactive HiPIMS deposition process

New international projects from RA1 and RA2:

- International scientific project between Institute of Physics CAS and Osaka University Japan focused on the research of thin film optical detectors
- M-ERA.NET project with EU partners (research institutions, industrial companies)
Smart industrial synthesis of transparent protective oxide thin films through plasma process control
- Horizon EU project with EU partners (research institutions, industrial companies)
Dr. Daniel Lundin and professor Henrik Pedersen, University of Linköping Sweden
“New plasma sources for CVD and ALD” (search for suitable call)

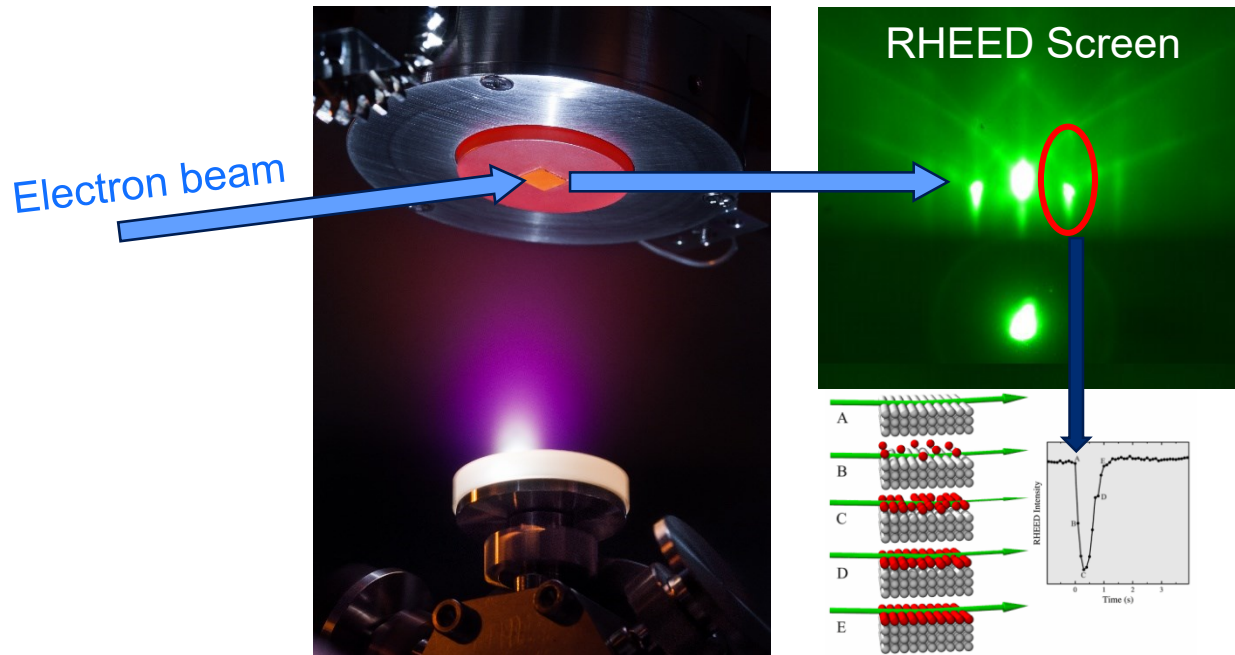
SOLID21

RA 3: Heusler alloys with outstanding magnetic and magnetooptic properties

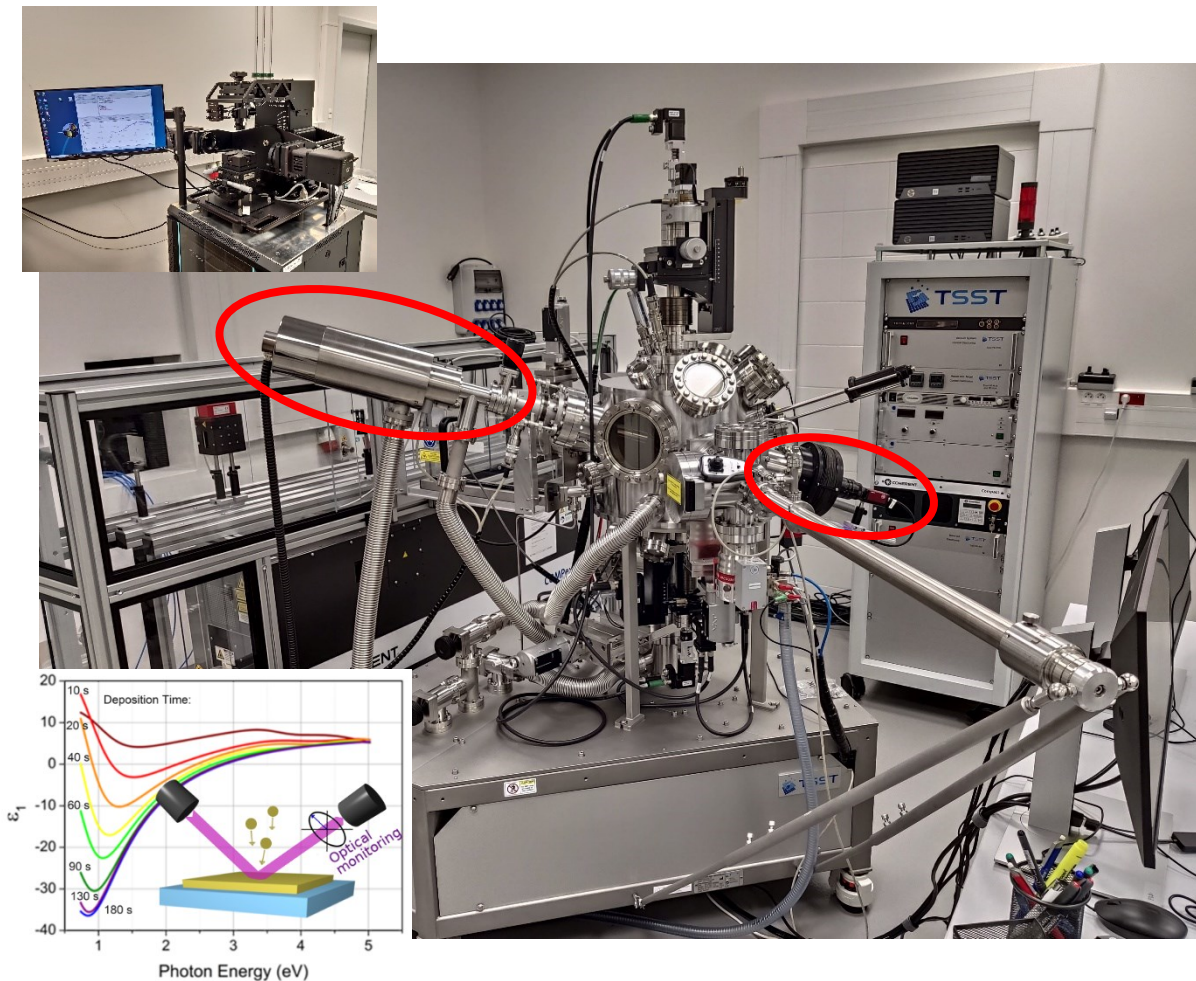
Ján Lančok

VP5-RA3-6

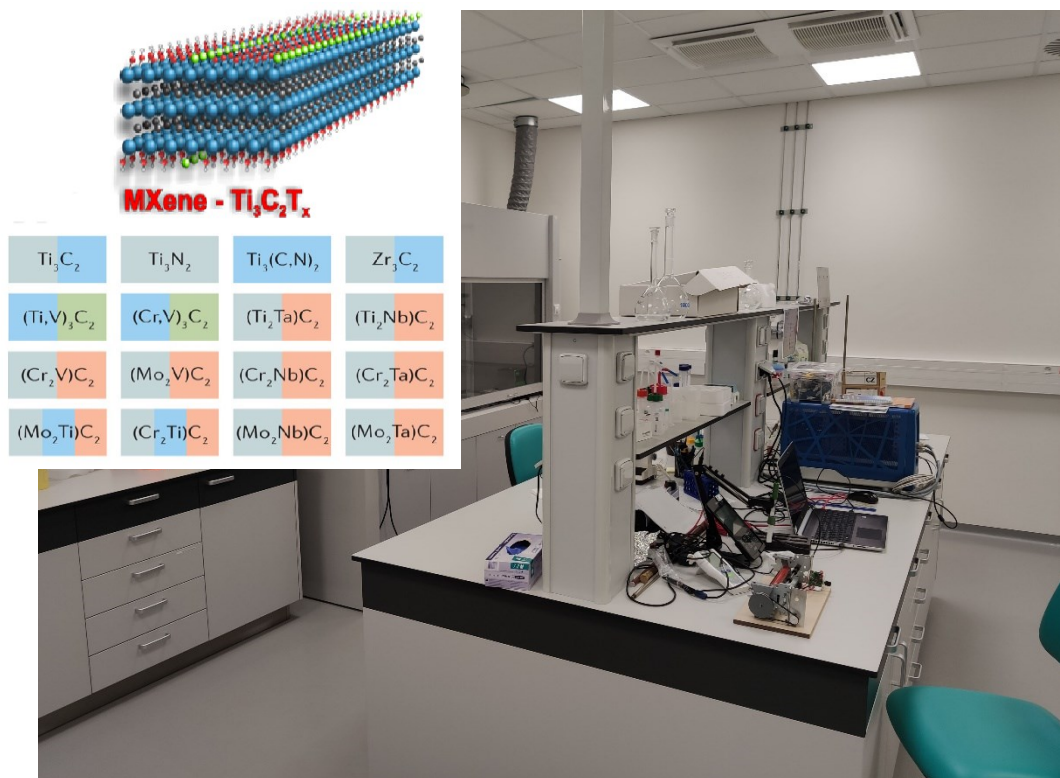
Pulsed Laser Deposition system with high pressure RHEED - Laser-MBE equipped with: in-situ ellipsometr, heating up to 1100°C, transfer under UHV for NanoESCA and STM



- Growing of high quality ferroelectric thin films such as SrTiO_3 , BaTiO_3
- Multiferroic system based on heterostructures MnO-NiO RA6 - (VP2)
- Heuller alloys Co_2TiSn for magnetooptics, Rh_2MnSb for spintronics RA3 - (VP1)
- Crystalline garnets and oxides doped with rare earth (VP3)



Laboratory for Mxene – 2D materials



Recently the great attention of the material community was paid on the family of 2D transition metal carbides, carbonitrides and nitrides (collectively referred to as MXenes).



M represents an early transition metal (such as Sc, Ti, Zr, Hf, V, Nb, Ta, Cr, Mo and so on),

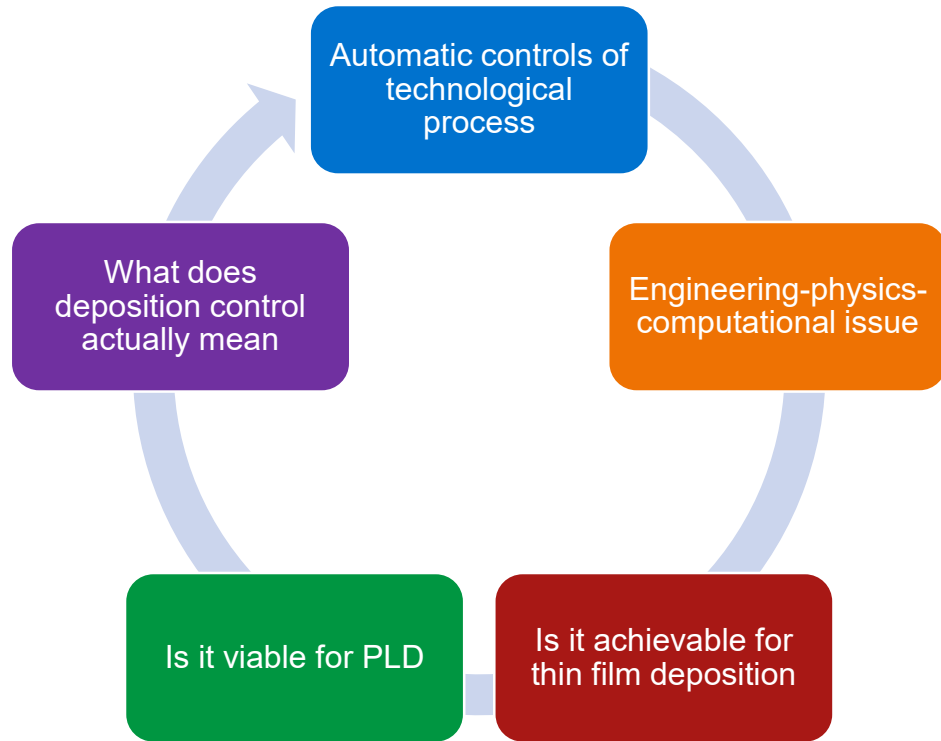
X is carbon and/or nitrogen and

T_x stands for the surface terminations (for example, hydroxyl, oxygen or fluorine).

Publications

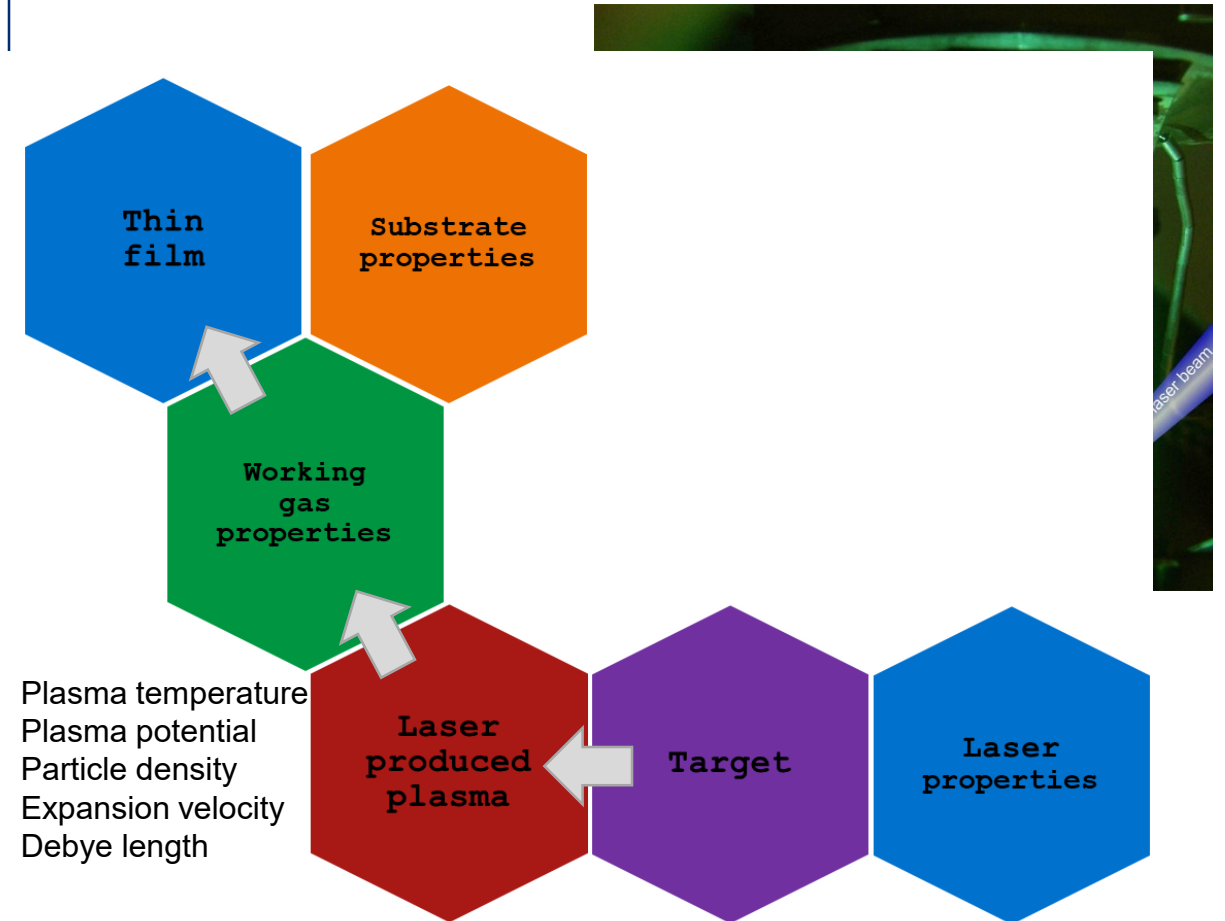
Plasmon coupling inside 2D-like TiB ₂ flakes for water splitting half reactions enhancement in acidic and alkaline conditions	Zabelina, A., Miliutina, E., Zabelin, D., (...), Švorčík, V., Lyutakov, O.	2023	Chemical Engineering Journal 454,140441
Chiral Plasmonic Response of 2D Ti ₃ C ₂ T _x Flakes: Realization and Applications <i>Open Access</i>	Olshtrem, A., Panov, I., Chertopalov, S., (...), Vana, J., Lyutakov, O.	2023	Advanced Functional Materials
Covalent functionalization of Ti ₃ C ₂ T _x MXene flakes with Gd-DTPA complex for stable and biocompatible MRI contrast agent	Neubertova, V., Guselnikova, O., Yamauchi, Y., (...), Chertopalov, S., Lyutakov, O.	2022	Chemical Engineering Journal 446,136939
Design of hybrid Au grating/TiO ₂ structure for NIR enhanced photo-electrochemical water splitting	Zabelin, D., Zabelina, A., Miliutina, E., (...), Švorčík, V., Lyutakov, O.	2022	Chemical Engineering Journal 443,136440
Plasmon-assisted MXene grafting: Tuning of surface termination and stability enhancement <i>Open Access</i>	Olshtrem, A., Chertopalov, S., Guselnikova, O., (...), Švorčík, V., Lyutakov, O.	2021	2D Materials 8(4),045037
Surface plasmon-polariton triggering of Ti ₃ C ₂ T _x MXene catalytic activity for hydrogen evolution reaction enhancement	Zabelina, A., Zabelin, D., Miliutina, E., (...), Chertopalov, S., Lyutakov, O.	2021	Journal of Materials Chemistry A 9(33), pp. 17770-17779

In-situ plasma diagnostics during PLD Toward the PLD automatiszation



Industry 4.0 is the digital transformation of manufacturing and related industries and value creation processes.

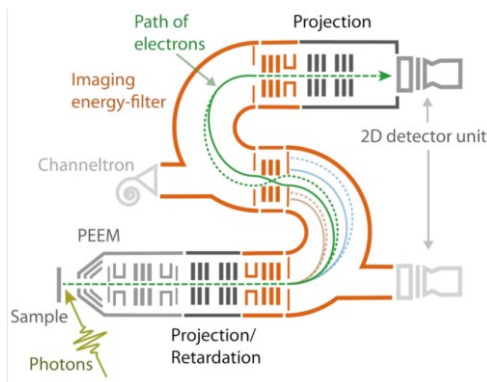
Langmuir probe method in its angular and time-resolved setup, combined with Optical em. Sp.



S.A. Irimiciuc et. al.

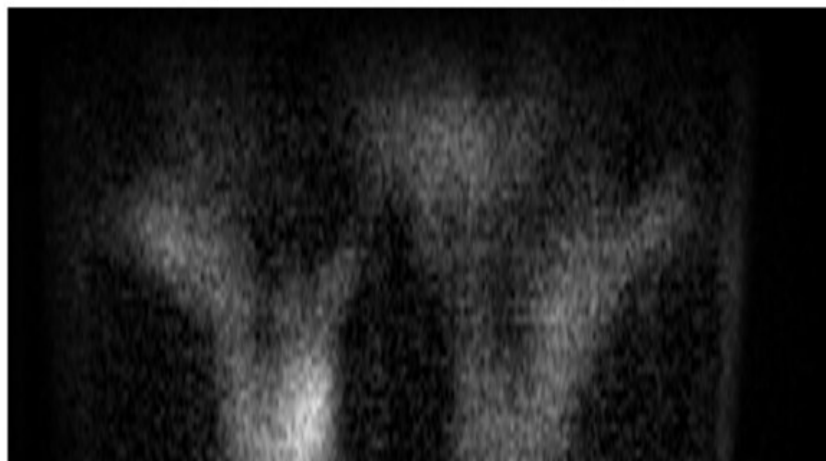
- Plasma Processes and Polymers e (2022) 2100102(1)-2100102(14).
- Vacuum 193 (2021) 110528(1)-110528(10)
- Coatings 11 (2021) 762(1)-762(17)
- Materials 14 (2021) 7336(1)-7336(13)

RA 3: Heusler alloys and thin metallic film –VP1

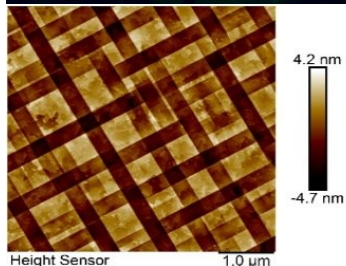
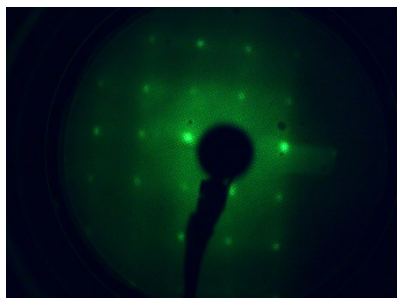


Rh₂MnSb 110 crystal direction

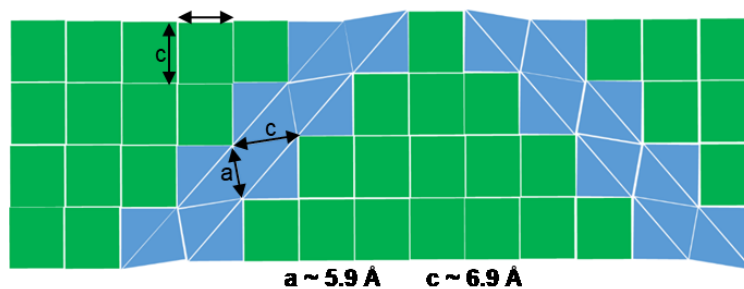
with background subtraction



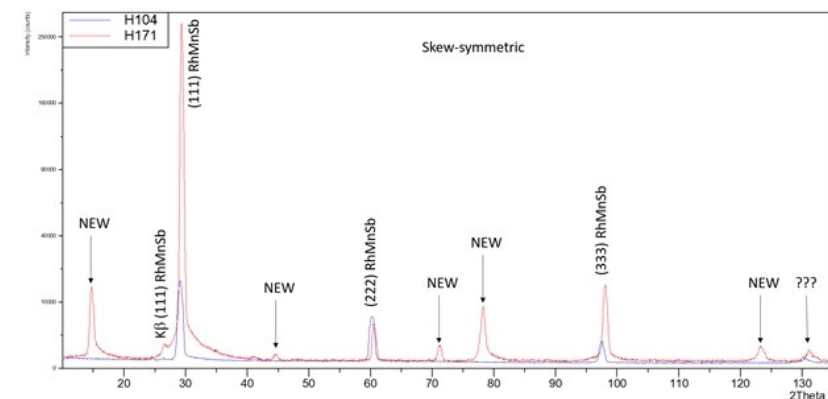
- UHV deposition chamber for magnetron sputtering
- UHV suitcase for transport to under UHV conditions to NanoESCA – XPS, ARPES



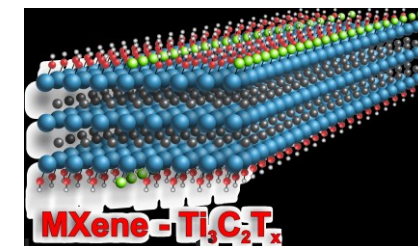
**Rh₂MnSb, RhMnSb,
Co₂TiSn**



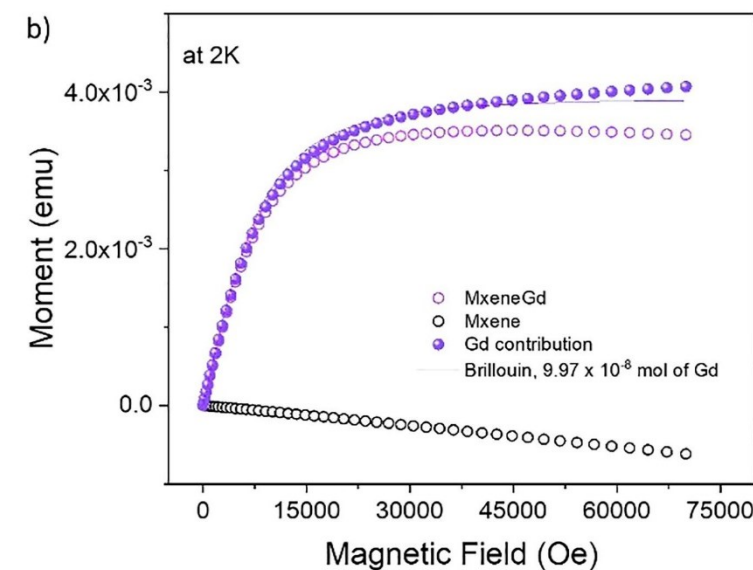
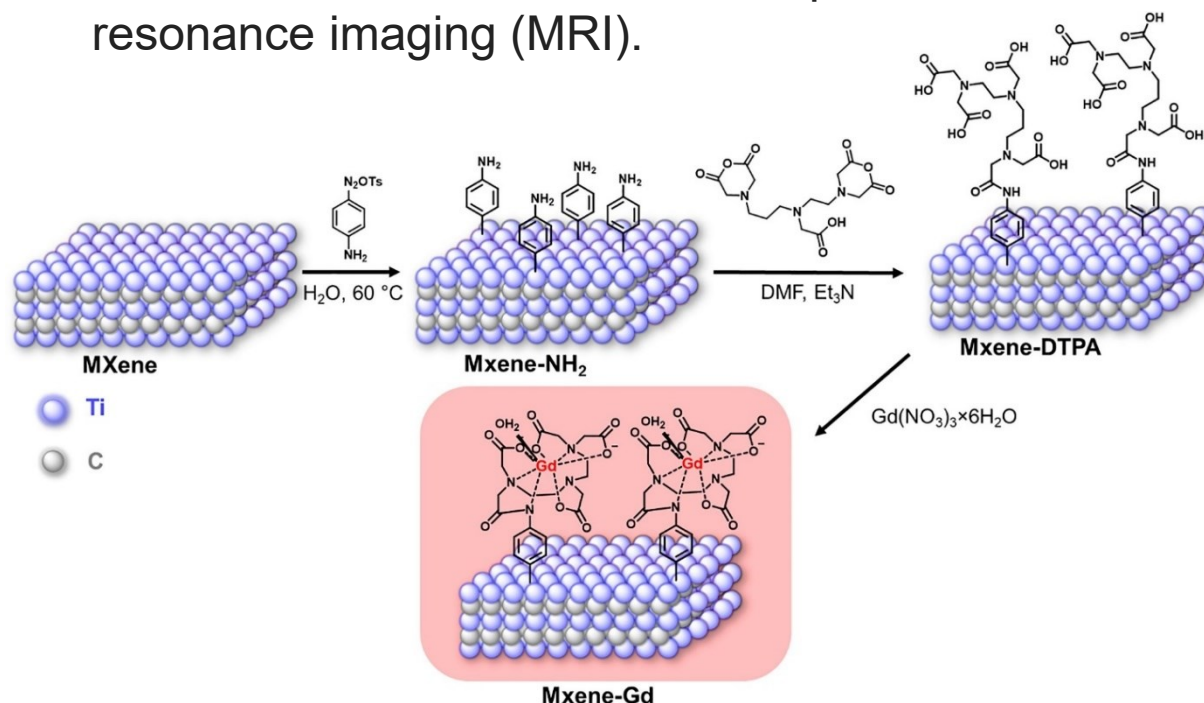
- Superstructural ordering of Heusler alloys PRB 105 (2022) 184106



Ti₃C₂ MXene films – plasmon-assisted surface modification and properties tuning



Modified MXene as a material for positron emission tomography, computed tomography, and magnetic resonance imaging (MRI).



paramagnetic

diamagnetic

- J. Lancok, S. Chertopalov, O. Lyutakov et al. Chemical Engineering Journal, 2022.



FZU

Fyzikální ústav
Akademie věd
České republiky

The project Solid state physics for the 21st century – SOLID21
CZ.02.1.01/0.0/0.0/16_019/0000760 is co-funded by the European Union.

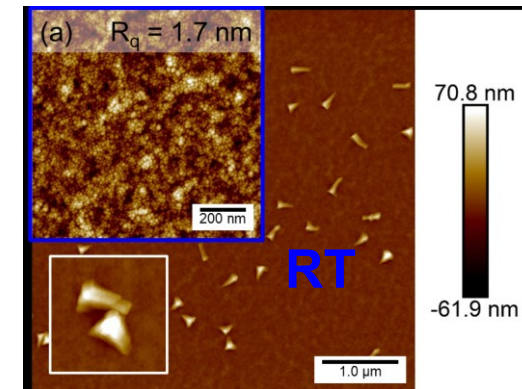
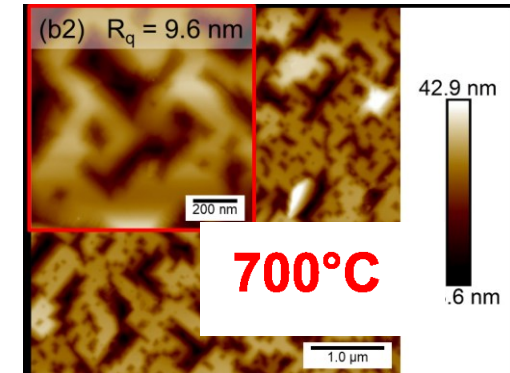
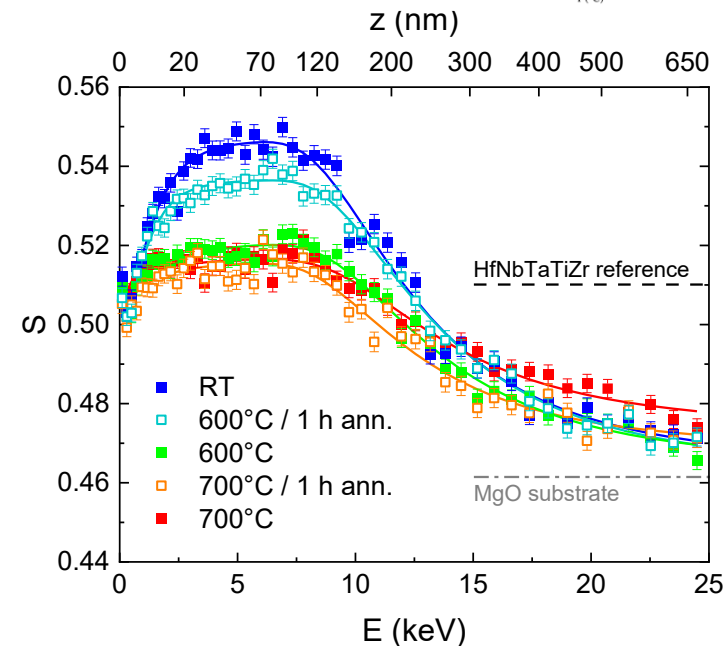
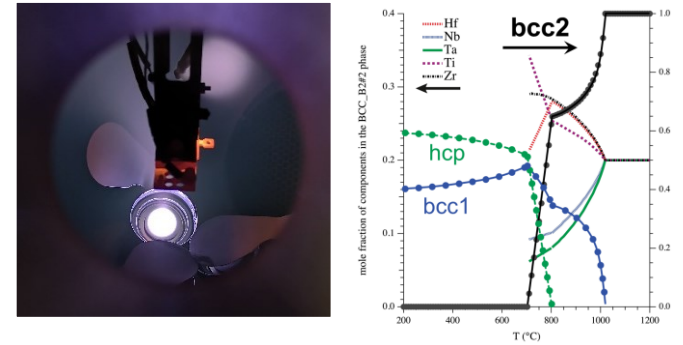
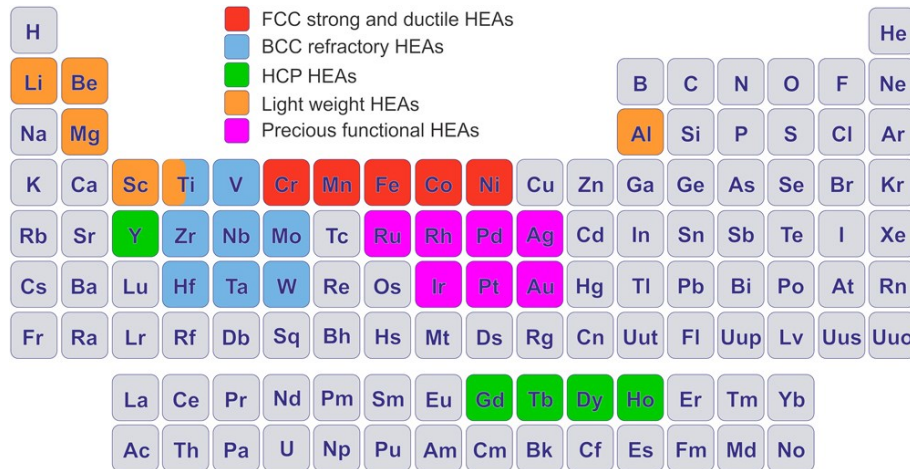


EVROPSKÁ UNIE
Evropské strukturální a investiční fondy
Operační program Výzkum, vývoj a vzdělávání



High-entropy Alloys (HEAs) thin films

HEAs represent a new type of materials with a unique combination of physical properties originating from the occurrence of single-phase solid solutions of numerous elements.

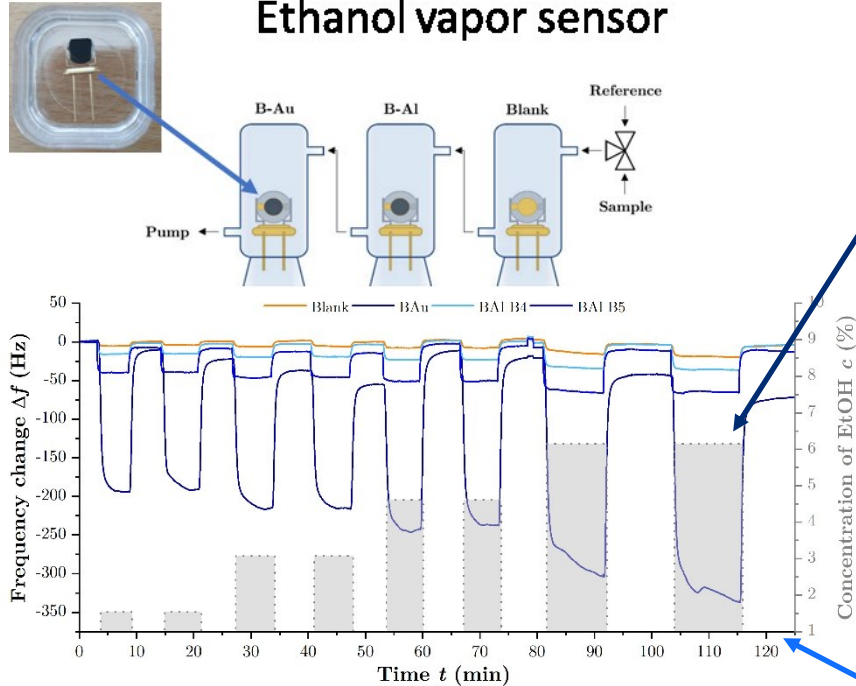


RA 4: Thin-film chemical sensors

Michal Novotný

Chemical sensors utilizing black metals

Ethanol vapor sensor



QCM	Sensitivity S	Sensitivity factor
Blank	2.1	1.0
B-Al 230 nm	4.0	1.9
B-Al 280 nm	5.3	2.6
B-Au 280 nm	21.3	10.2

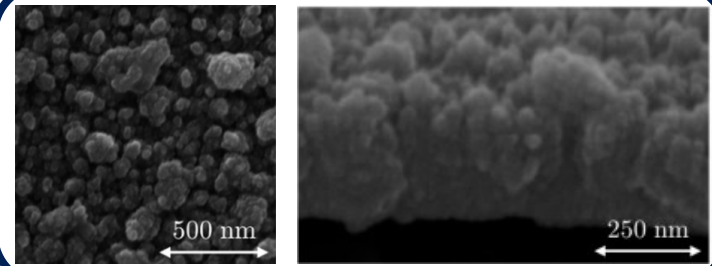
M.Hruška et al., Nanomaterials, 2022, 12, 4297



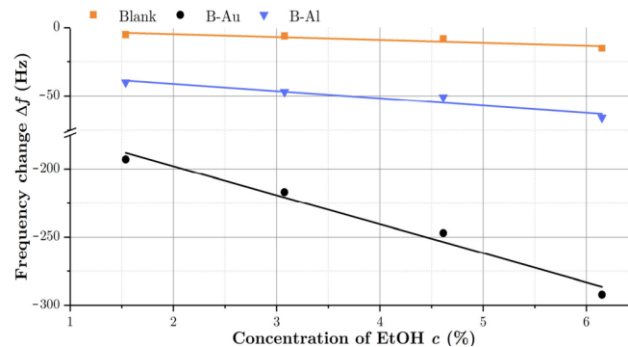
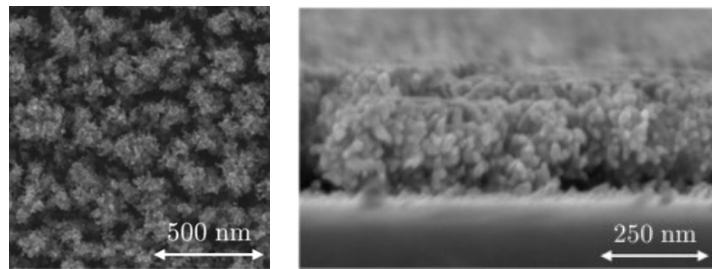
FZU

Fyzikální ústav
Akademie věd
České republiky

Black Al –DC pulsed magnetron sputtering



Black Au – thermal evaporation

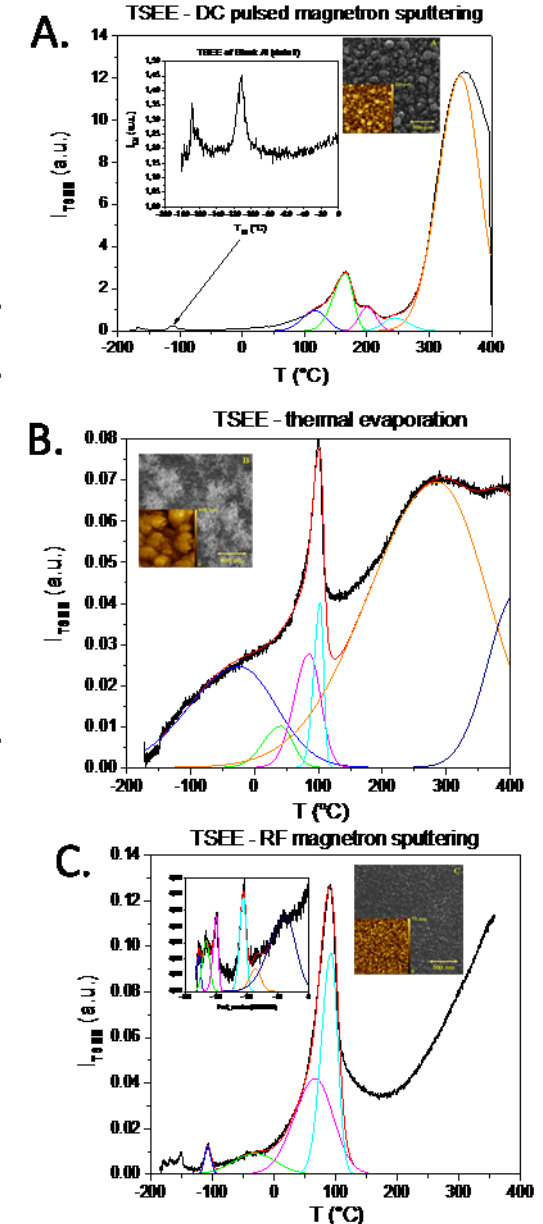


Black Al surface el. structure studies
thermostimulated exo-electron emission (TSEE)

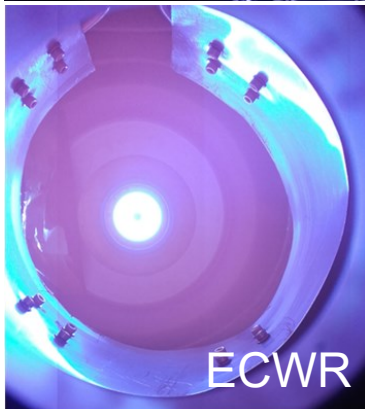
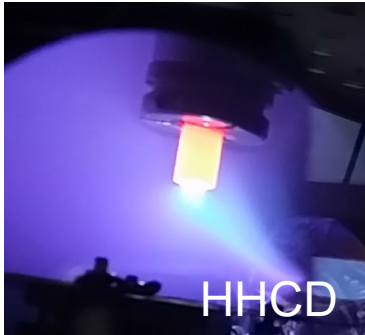
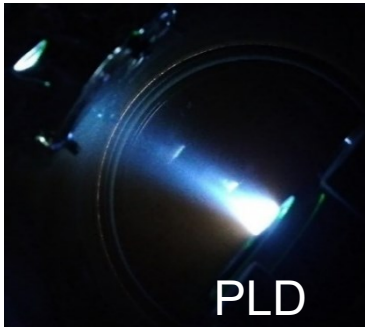
sample		A	B	C
T_{m1}	°C	166.1	102.7	91.7
T_{m2}	°C	349.2	286.8	
I_1	a.u.	2.83	0.04	0.13
I_2	a.u.	12.15	0.07	
E_1	eV	0.95	0.81	0.79
E_2	eV	1.34	1.2	

$E_{1,2}$... determined activation energies

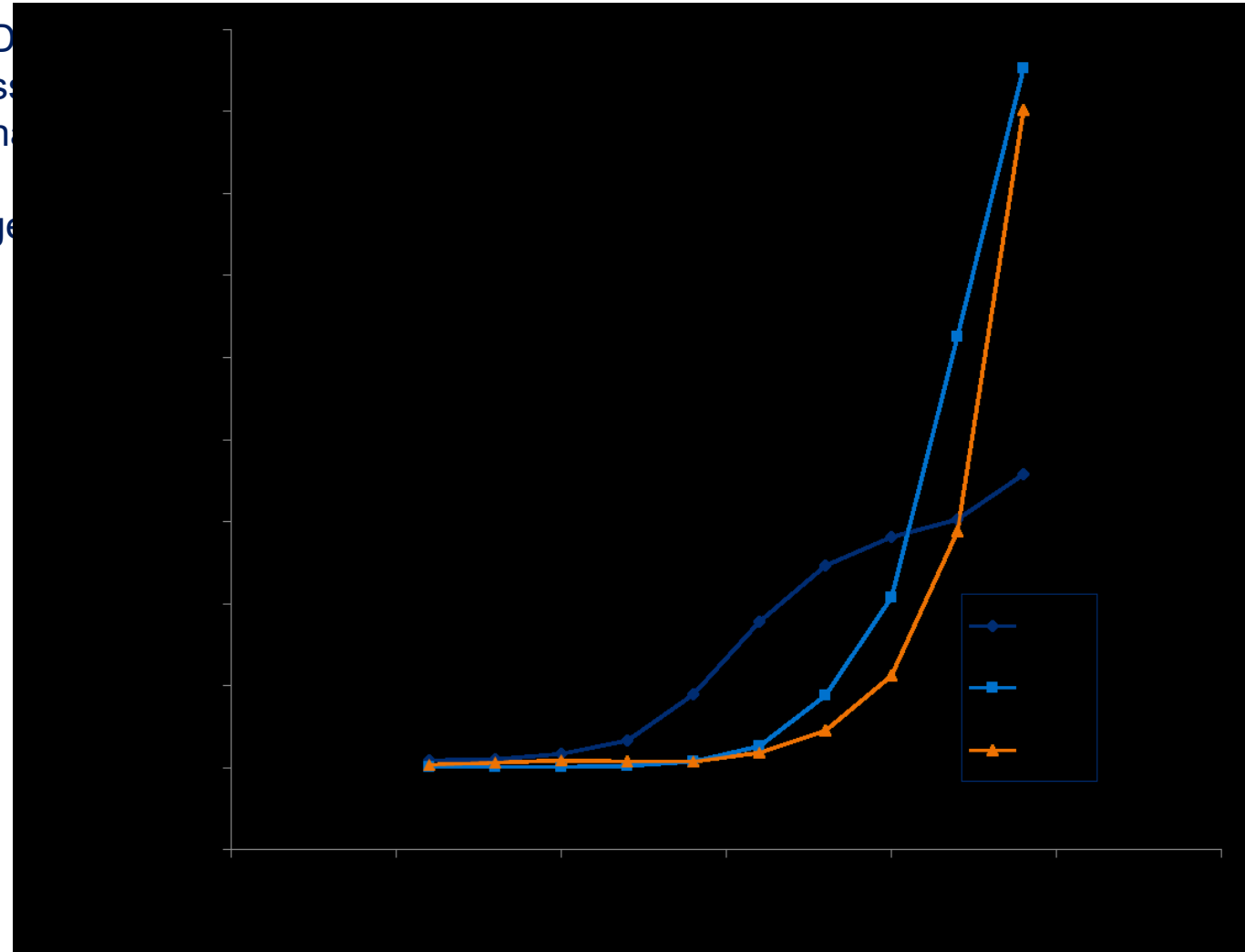
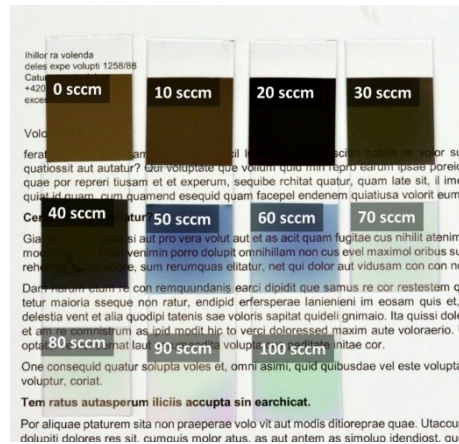
Black Al
PVD techniques and surface properties



WO₃ Thin-film chemical sensors all VP5



- Pulsed Laser Deposition (PLD)
- HiPIMS reactive sputtering as well as electron cyclotron wave resonance plasma (ECWR)
- Hot Hollow Cathode Discharge



Invited lecture of EMRS 2023:

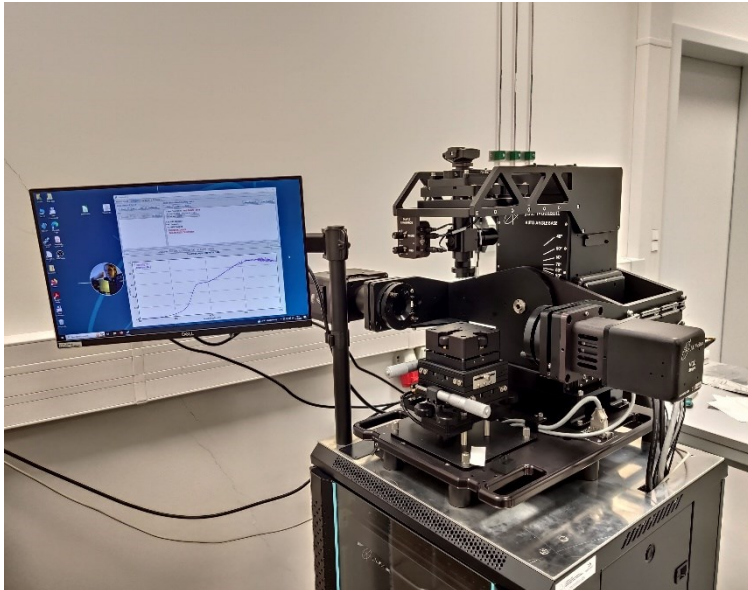
J. Lančok, Tungsten oxide thin films fabricated by PLD, HiPIMS and DC hollow cathode discharge for chemical sensor.

RA 5: Optical materials-plasmon structures

Jiří Bulíř

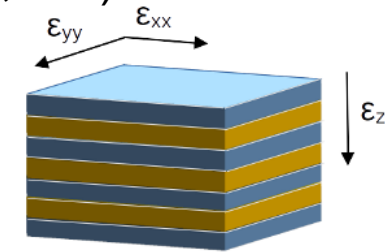
Optical materials-plasmon structures

In-situ spectral ellipsometer (J.A.Woollam, M2000):
monitoring of the growing films

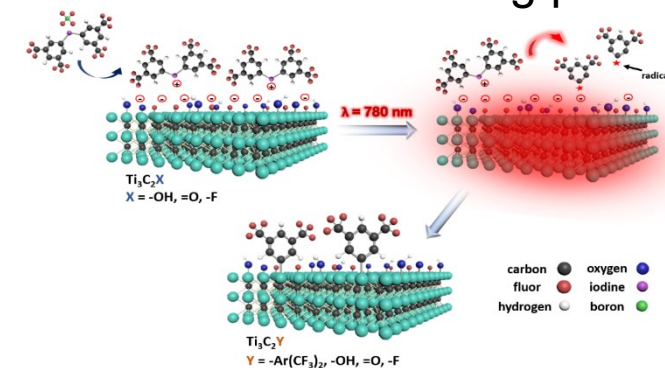
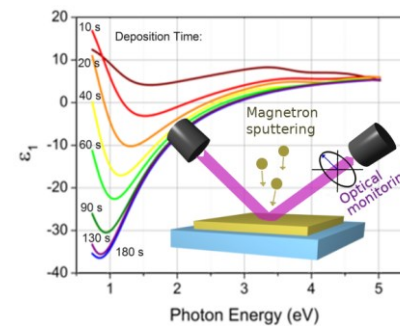


Optical dielectric functions can be obtained during the deposition process. The development of the dielectric function during the ZrN layer growth can be seen.

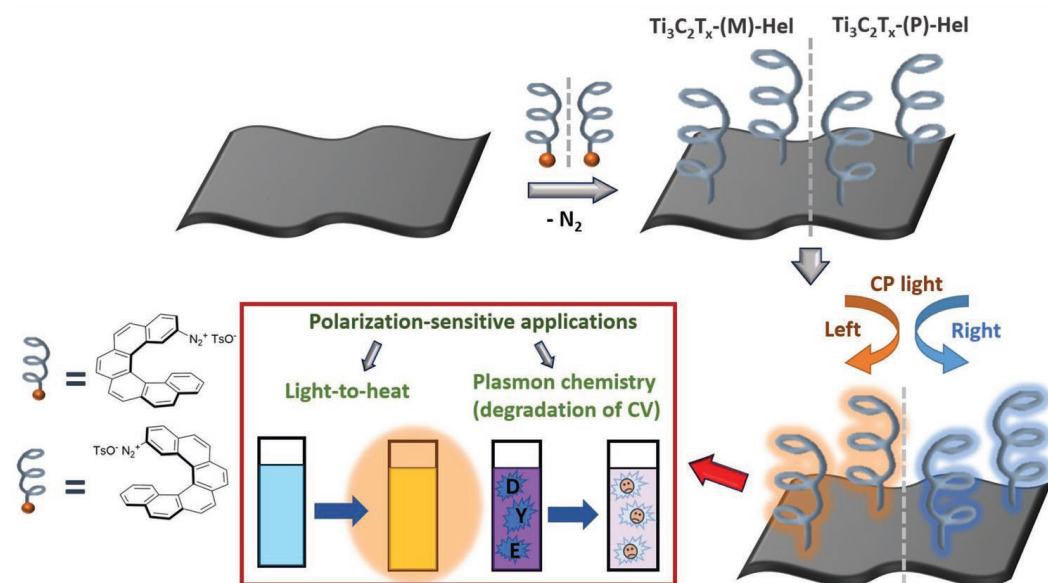
Materials characterized by extreme anisotropy - it is formed as a layered structure of ultrathin epitaxial dielectric (ScN,CrN) and metallic film (TiN,ZrN)



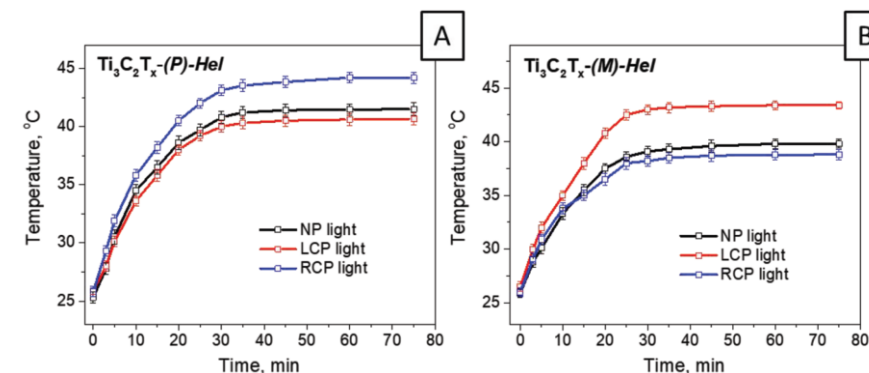
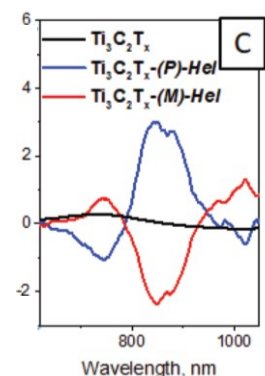
MXen materials with outstanding plasmonic behavior



Chiral Plasmonic Response of 2D $\text{Ti}_3\text{C}_2\text{T}_x$ Flakes



Circular dichroism



Demonstration of potential chiral 2D flakes utilization: Plasmon-induced heating

RA 6: Structures exhibiting combinations of ferroelectric and ferromagnetic properties

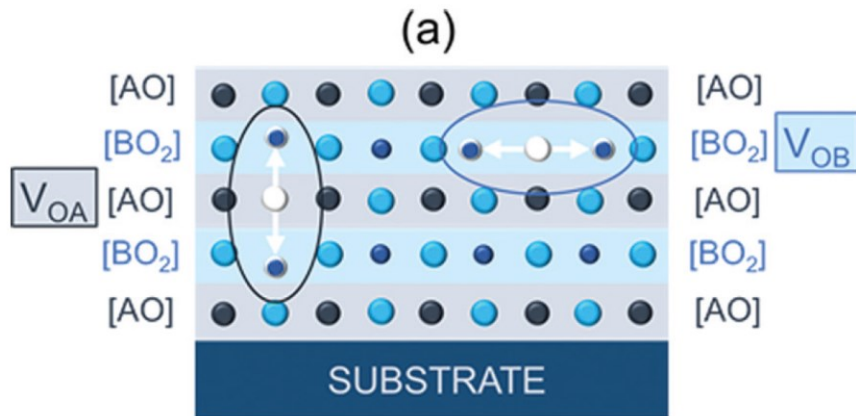
Maria Tyunina

Fabrication of epitaxial perovskite oxide films by PLD and tailored properties by defect and by thermal strain an oxygen vacancies

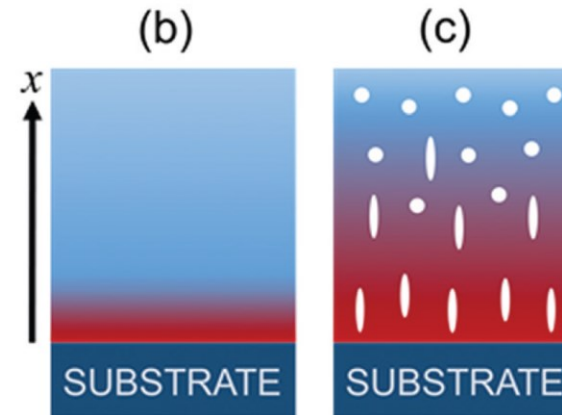
By PLD (KrF laser) thin (Th ~ 100 nm) films of:

- SrTiO_3
- BaTiO_3
- NaNbO_3
- $\text{K}_{0.5}\text{Na}_{0.5}\text{NbO}_3$
- $\text{Ba}_{0.5}\text{Sr}_{0.5}\text{TiO}_3$

- Anisotropic lattice distortions around oxygen vacancies are intrinsically inherent to all perovskite oxides.
- Therefore, we anticipate that the interaction of oxygen-vacancy stresses with substrate-induced strain fields is general for epitaxial perovskite oxide films.

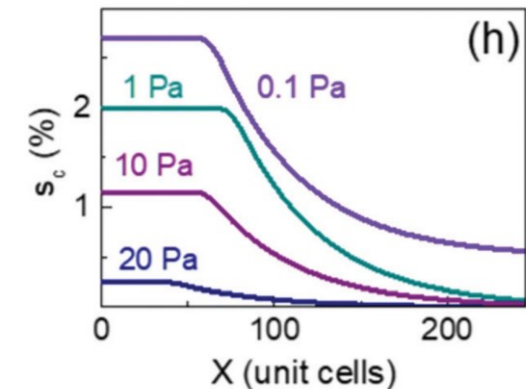


Schematics of exaggerated displacements of B-cations around oxygen vacancies in different atomic planes.



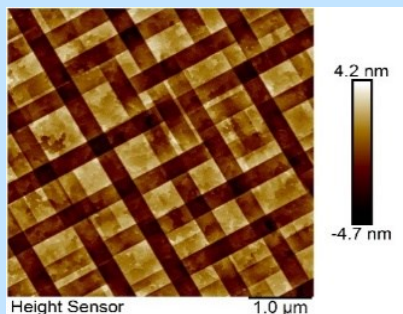
Stoichiometric

Oxygen-deficient films



Model strain profiles from the XRD peaks in as a function of the distance x from the film-substrate boundary

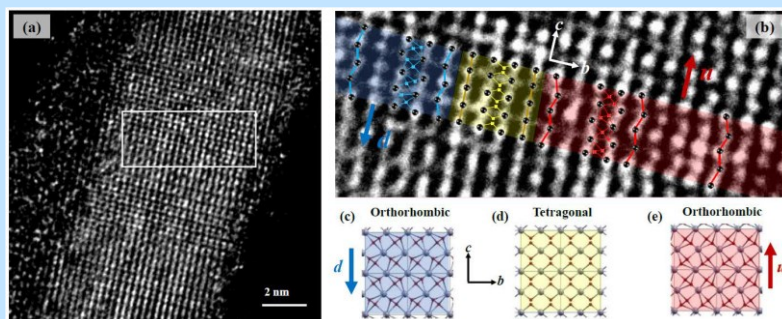
VP1 – Heusler thin films



Rh_2MnSb
 RhMnSb
 Co_2TiSn

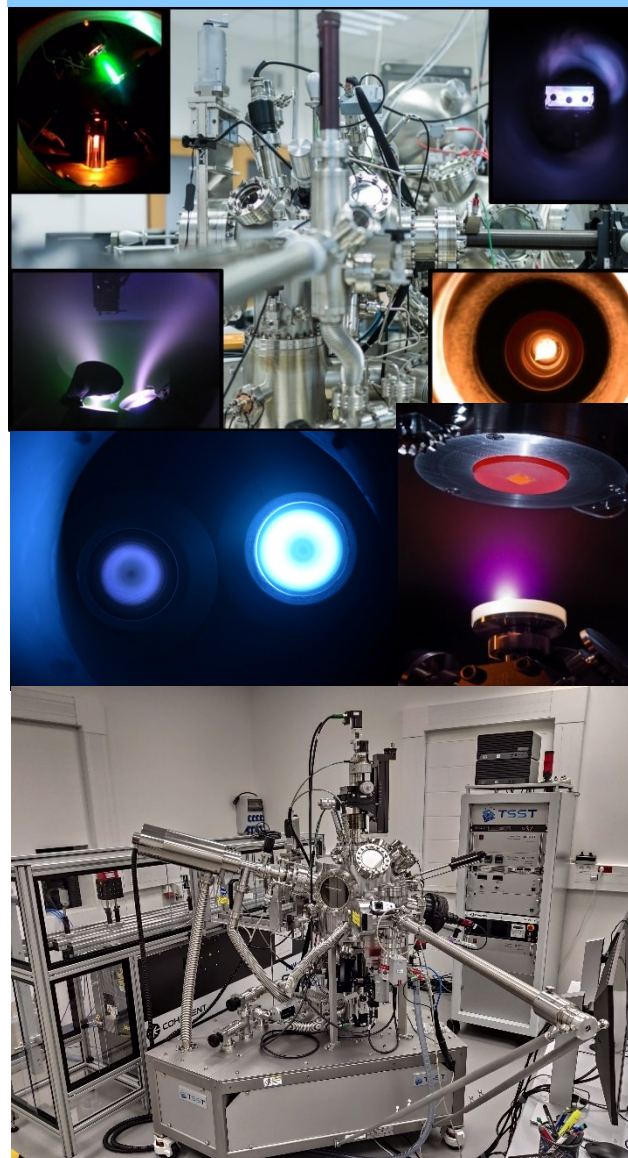
V. Chab, Effect of Twinning on Angle-Resolved Photoemission Spectroscopy Analysis of $\text{Ni}_{49.7}\text{Mn}_{29.1}\text{Ga}_{21.2}(100)$ Heusler Alloy, *Materias* 717 (2022)

VP2 – Ferroelectrics films HfO_2 Multiferroic films

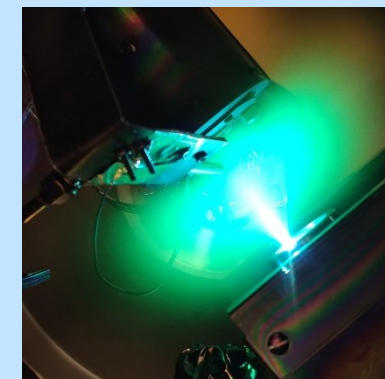


A. Kashir, *Nanotechnology* 33 (2022) 155703

VP5- Plasma technology

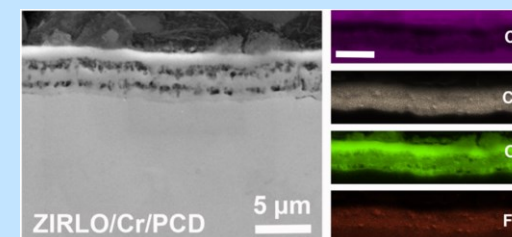


VP3 – oxides, iodines, garnets



I. Irimiciuc, Investigations on the CuI thin films production by pulsed laser deposition, *Applied Surface science* 606 (2022)

VP4 - Diamond group, microwave plasma and diamond thin films characterisation



I. Kratochvilova, Polycrystalline diamond and magnetron sputtered chromium as a double coating for accident-tolerant nuclear fuel tubes, *Journal of Nuclear Materials* (2023)

Influence of SOLID 21

International cooperation and

- V4+ Japan project focused on black metals for chemical sensors
- Royal Chemical Society with University Exeter UK - Mxene under dynamic strain
- Mobility project with University in Tartu, Estonia – chemical sensors

✓ Integration of SOLID laboratories to our current infrastructure

Year	Number of publications	Q1	IF average	FTE
2017-18	59	24	4.2	25.1
2022-23	56	32	6.2	22.3

Sustainability

- M-ERA.NET project with EU partners (research institutions, industrial companies) Plasmon-Enhanced Nanostructured Optical Transparent Detectors ,
- NATO program (partner EXCALIBUR ARMY s.r.o.) - Stealth coatings based on 3D architectures of high entropy materials
- LA –Slovenia *Refractory high entropy alloy thin film photoelectrocatalyst: from synthesis to pharmaceutical wastewater treatment (RHEATREAT)*
- *TACR 2 project with TESLA, 7 GACR*
- *One MCSA – CZ*
- *Participation in COFUND project*

Cooperation with industry

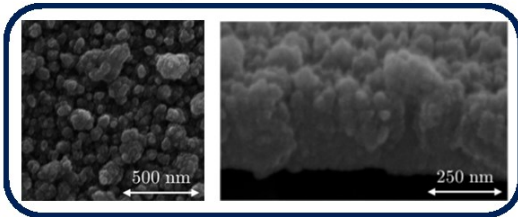
Basic research

Publications

Application project

Commercial outcomes

Black Al –DC pulsed magnetron sputtering



nanomaterials



Article

Surface Enhancement Using Black Coatings for Sensor Applications

M.Hruška, 2022, 12, 4297



Commercialisation of black metals films with Switzerland company



Metal oxide chemical sensors



THE JOURNAL OF
PHYSICAL CHEMISTRY C

Cite This: J. Phys. Chem. C 2010, 123, 29739–29749

Article
pubs.acs.org/JPC

New Insight into the Gas-Sensing Properties of CuO_x Nanowires by Near-Ambient Pressure XPS

P. Hozak, 2020

MPO
PROGRAM TRIO

Method of applying layers on sensor platforms for detecting gas

Patent number: 309041



Cooperation with industry

Basic research



Publications

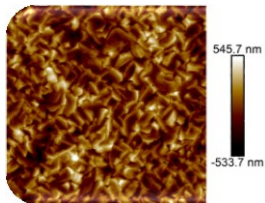


Application project



Commercial outcomes

High-entropy Alloys



Oxidation of amorphous HfNbTaTiZr high entropy alloy thin films prepared by DC magnetron sputtering
P. Hruska, 2021

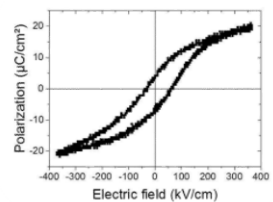


Stealth coatings based on 3D architectures of high entropy materials

K	Ca	Sc	Ti	V	Cr
Rb	Sr	Y	Zr	Nb	Mo
Cs	Ba	Lu	Hf	Ta	W
Fr	Ra	Lr	Rf	Db	Sg



Perovskite oxide films PZT



RESEARCH ARTICLE | DECEMBER 22 2015
Magnetoelectric coupling in Pb(Zr,Ti)O₃—Galfenol thin film heterostructures ✓
J. More-Chevallier; U. Lüders; C. Cibert; ... et. al



Program **Trend**

Lithographic ultrasonic arrays from smart materials for Industry 4.0

Functional sample - SONOPOLYMERS WITH SMART MATERIALS FOR SONOLITHOGRAPHY





Thank you for your attention.